ROBOMINERS DELIVERABLE D2.1

REPORT ON LABORATORY TESTS ON EARLY STAGE ALTERNATIVE PROTOTYPES ON LOCOMOTION, SENSING AND NAVIGATION IN MINING ENVIRONMENTS

Summary:

This deliverable looks at the work progress with scale lab prototypes on locomotion, sensing and localization of the first half of the ROBOMINERS project and reports the early-stage results within each of the fields. The reported work is ongoing and will be continued after the submission of this deliverable.

The built test environments, experimental lab scale platforms and test rigs will contribute to future work and lay base for software development and testing within WP4, help to test and validated the concepts for WP3/WP7 and set ground for the initial work of selective mining within WP6.

The reported work within this report was affected by the COVID-19 crisis, that limited the access to the labs for some partners and most of all, hindered cooperation among partners developing physical prototypes.
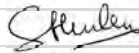
Authors:

Asko Ristolainen, TalTech, WP participant
Laura Piho, TalTech, WP participant
Roza Gkliva, TalTech, WP participant
Simon Godon, TalTech, WP participant
Claudio Rossi, UPM, Project coordinator
Christian Burlet, RBINS, Project participant
Giorgia Stasi, RBINS, Project participant
Eetu Friman, TAU, Project participant
Raphael Goossens, TAU, Project participant
Kalle Hakonen, TAU, Project participant
Pirkka Ulmanen, TAU, Project participant
Virgilio Gomez, UPM, Project participant

Title:	Report on laboratory tests on early-stage alternative prototypes on locomotion, sensing and navigation in mining environments.
Lead beneficiary:	TalTech
Other beneficiaries:	TAU, UPM, RBINS
Due date:	01.06.2021
Nature:	Confidential
Diffusion:	all Partners
Status:	Draft
Document code:	

Revision history	Author	Delivery date	Summary of changes and comments
Version 01	AR et al	30.06.2021	
Version 02			
Final version			

Approval status				
	Name	Function	Date	Signature
Deliverable responsible	Asko Ristolainen		05.07.2021	
WP leader				
Reviewer	Stephen Henley	QC	01.07.2021	
Reviewer	Sergio Domínguez	QC	02.07.2021	
Project Coordinator	Claudio Rossi		02.07.2021	

This document reflects only the author's view and the European Commission is not responsible for any use that may be made of the information it contains.

TABLE OF CONTENTS

TABLES

FIGURES

Executive summary

This deliverable looks at the work progress with scale lab prototypes on locomotion, sensing and localization of the first half of the ROBOMINERS project and reports the early-stage results within each of the fields. The reported work is ongoing and will be continued after the submission of this deliverable. The built test environments, experimental lab scale platforms and test rigs will contribute to future work and lay base for software development and testing within WP4, help to test and validated the concepts for WP3 and set ground for the initial work of selective mining within WP6.

The reported work within this report was affected by the COVID-19 crisis, that limited the access to the labs for some partners and most of all, hindered cooperation among partners developing physical prototypes.

1   INTRODUCTION: DEVELOPMENT AND EXPERIMENTATION

Within this deliverable we report the research on alternative designs shown in D1.1 (Ristolainen, Piho, and Kruusmaa 2020) and D1.2 (Ristolainen, Kruusmaa, and Godon 2020), but also testing concepts of the final miner prototype developed in WP3 and presented in D3.2 (Aaltonen et al. 2020). The report also demonstrates early lab experiments done with sensing following perception techniques, listed in D6.1 (Burlet et al. 2020). The reported work in this deliverable shows the results by M24 and will be continued after the submission of this deliverable.

The built test environments, experimental lab scale platforms and test rigs will contribute to future work and lay base for software development and testing within WP4 and set ground for the work of selective mining within WP6. The lab scale prototypes help to test and validated the concepts for WP3 and WP7. The development and experimentation will follow the operational scenarios presented in (WP4 2021), that distributes the development and demonstrations between different prototypes, lab demonstrations and simulations (see Table 1).

Table 1 ROBOMINERS scenarios and implementation platforms

No.	Scenario Name	RM1	RM2	RM3	RMS1	RMS2	RML
1	Go to location	*	*	*	*	*	
2	Ore extraction	*			*	*	*
3	Power assurance	*			*	*	*
4	Fault detection	*	*		*	*	*
5	Reconfiguration	*	*		*	*	
6	Self-assemble					*	
7	Mine mapping	*	*	*	*	*	*

RM1: Full scale robot (TAU)
RM2: Small scale robot (UPM)
RM3: Small scale robot (TalTech)
RMS1: simulator
RMS2: simulator
RML: lab demonstration

2 LOCOMOTION

The main challenge for locomotion in mining environments is the uncertainty of soil and surface type where the robot needs operate. Slurry and wet environments are common in underwater mines, in some cases also underwater conditions can be found as for abandoned mining scenario described D5.1 (Hartai et al. 2020) . For the robust robot design presented within D3.2 (Aaltonen et al. 2020), locomotion principles were evaluated in soil-screw interaction experiments. Additionally, alternative design studies are presented along with a re-configurability platform for fault management.

2.1 EXPERIMENTAL LAB TEST POOL AT TAMPERE

For testing the ROBOMINERS locomotion system (the screw-leg system) with laboratory (small) and actual size system a test pool size with a size of ∅3,6 m and height is 1,2 m was assembled. The test pool was built on using a swimming pool, with additional supporting inner thicker plastic canvas to prevent ruptures of the main pool canvas. The pool is filled with a layer of 50 mm thick EPS plate, a layer of sand and three different mediums on top of the sand (Figure 1).

Figure 1 Different pool filling steps and the 5th shows how the mediums are divided inside to the pool

Three different mediums are in the pool are:
- sand
- gravel (0 – 30 mm)
- rough gravel
- concrete plate to imitate hard surfaces like walls of tunnel.

These mediums where selected based on research of rock sizes in the excavation tunnel when drilling or grinding or blasting rock in smaller scale. These mediums are divided in three different sections in the test pool. Additionally, water can be added to the pool to make slurry from the sand to investigate how the medium's density affects the locomotion.

Test rig

For measurements inside the test pool is test rig shown in Figure 2. This test rig has braking disc, distance meter and a force gauge. The automation is made with Beckhoff automation system. A wire is connected to the force gauge to provide at the same time pulling force and distance that the prototype has travelled. The distance measurement unit can measure distance up to 2000 mm and the force gauge is capable to measure 1000 N. There is also own measurement unit for measuring voltage and amperes of electrical motor. All the data is collected via computer data file which can be read with excel etc. to

make analysis. Figure 3 shows sample visualization of the plotting. This rig is scalable for a bigger screw; it needs only to change the force gauge and increasing the break force.

The work principle

When the robot starts to move and starts pulling the distance measurement unit wire the brake starts to break little by little as the robot moves forward. When the robot stops then we have achieved maximum pulling force that the robot can provide. Same time the computer draws different plots from velocity, distance and force.
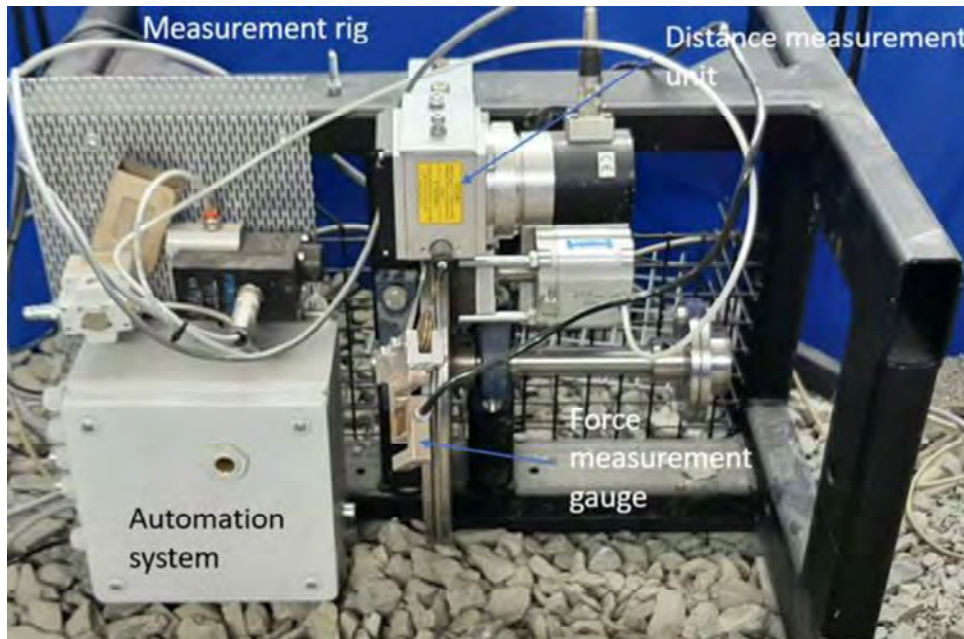
Figure 2 Overview of the test rig
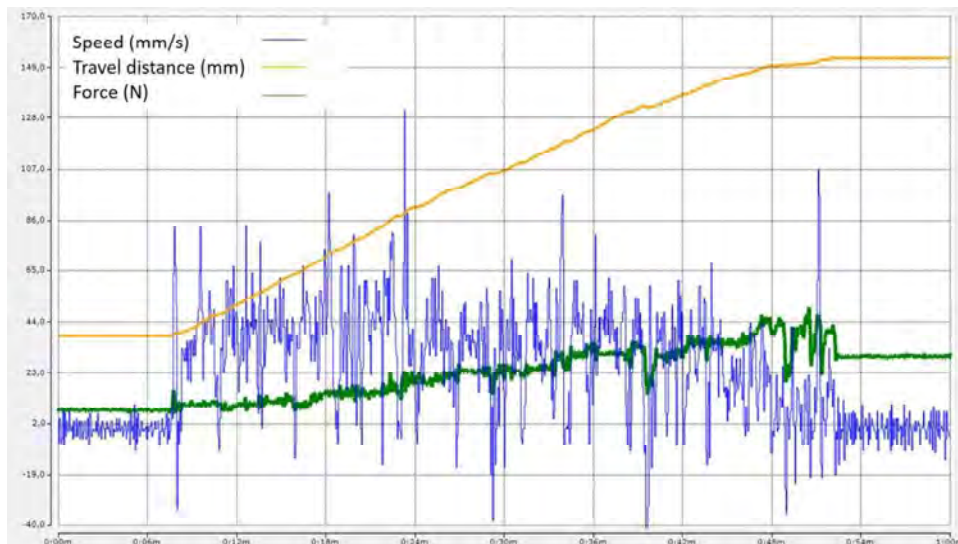
Figure 3 Sample plotting from test rig visualization

2.2 SOIL-SCREW INTERACTION EXPERIMENTS AT TALTECH

The soil-screw experiments at Taltech were aimed at evaluation of the forces, torques and speed relations to the RPM of the screw driven locomotion module and the dependence of the kinematics of different loading and surface conditions. The experiments were conducted with a screw actuator developed in TalTech, that uses two individually controlled counter-rotating screws in one module to reduce lateral forces. The screw actuator described in D3.2 ((Aaltonen et al. 2020) - Appendix 4 in D3.2) is a simplified case of the design shown in Figure 4, where the actuating linear thrust force is a sum of two screws.
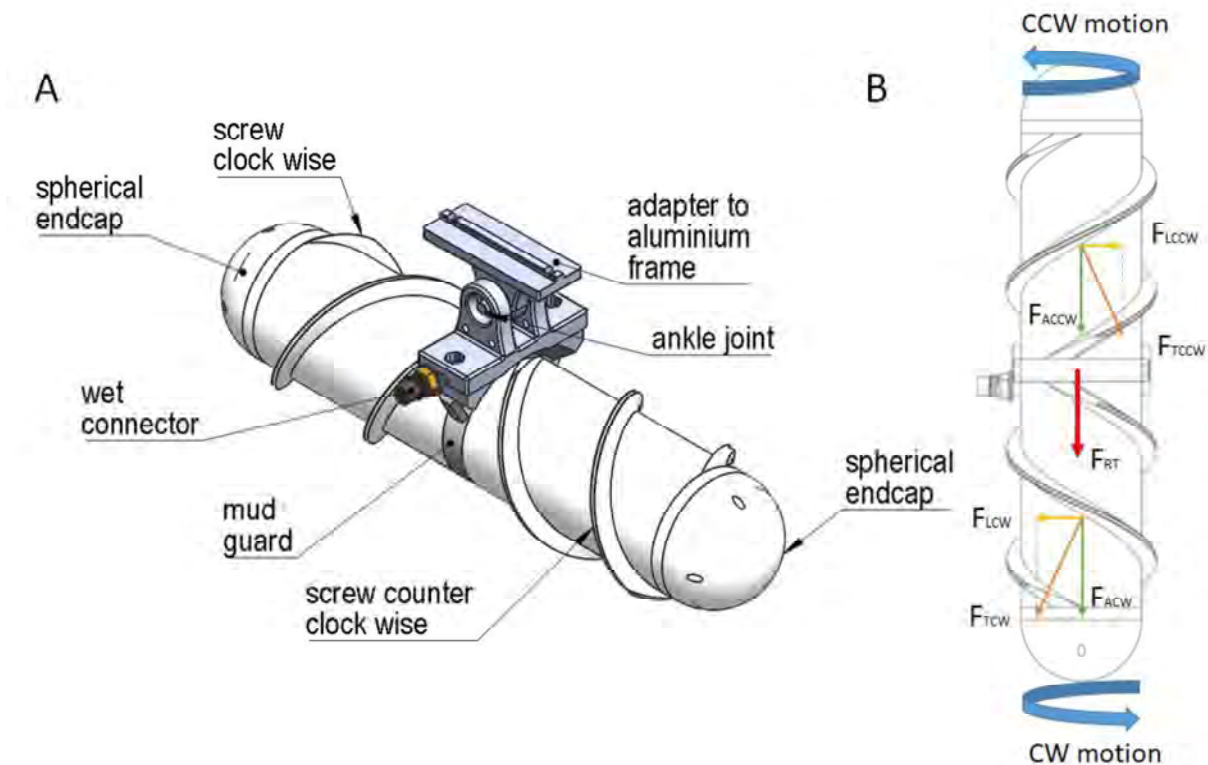
Figure 4 Screw module with two actuated screw sheaths; B: Thrust forces of the counterclockwise (CCW) and clockwise (CW) screws (L – lateral, A – axial, T – total thrust, RT – resultant thrust)

Experimental setup

The experiments were performed on the testbed presented in figure 5 below. It consists of a test tank whose bottom is filled with concrete with large asperities to simulate the hard bottom of a mine, and covered with different materials that can be covering the bottom of a mine tunnel:
- **Gravel** (particle size: 2-6 mm)
- **Dry sand** (particle size: 0.1 - 2 mm)
- **Wet sand** with 80%-100% humidity (particle size: 0.1 - 2 mm)

The screw actuator is mounted on a gantry that enables translation and rotation of the actuator along the longitudinal axis (direction of motion). Following parameters were measured in the setup:
- **Forces and torques (F/T)** – ATI Axia80 M20, serial connection, 100 Hz.
- **Movement speed** – time-of-flight sensor, VL53L0X, 40Hz (each measurement takes about 25ms), the linear velocity of the actuator is estimated in post-processing, by differentiating the position information obtained with this sensor.
- **Current measurements** – LEM LTSR 6-np, 100Hz
- **RPM of the motor** – internally calculated from motor encoders with Arduino Nano (10 ms)

- **Sinkage** – TE 571-G-NSDOG1-022 inclination sensor, serial 100 Hz, measured from the rotation around the linear guide

The data acquisition was performed using a Windows PC running a custom MATLAB/Simulink program using Desktop Real-Time in external mode. Data acquired include motor angular velocities, forces and torques, current consumption, the tilt angle of the actuator mounting plate, distance of the actuator from the tank wall (ToF sensor), along with information on experiment conditions and actuator parameters for each dataset.
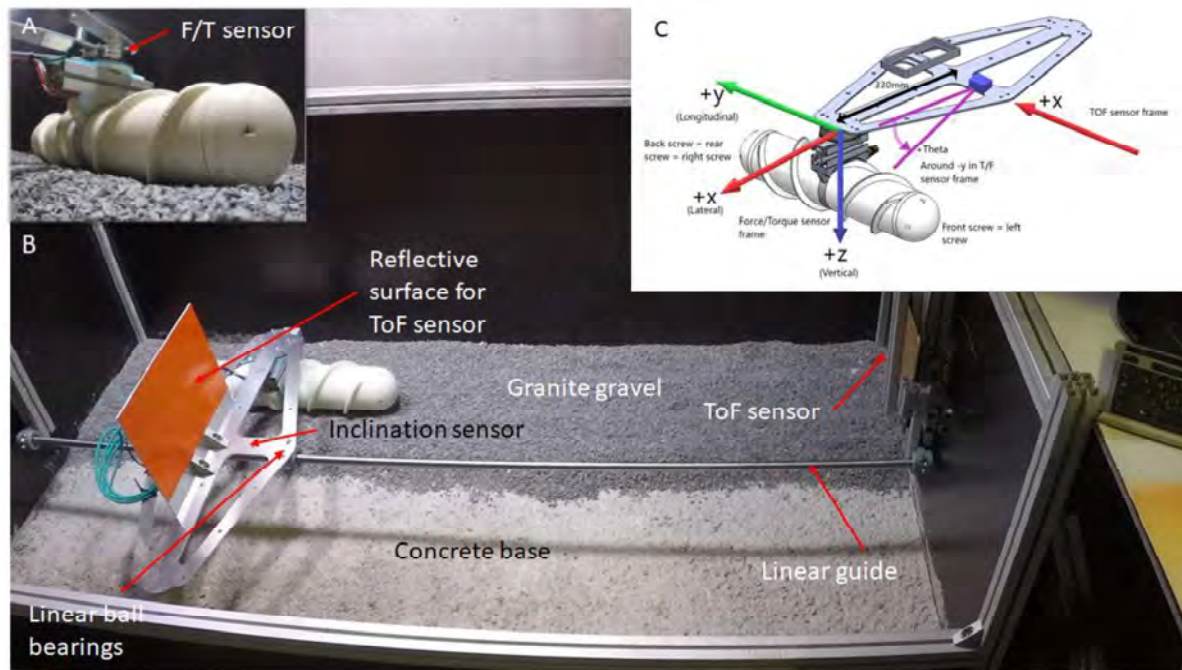
Figure 5 A: Positioning of the F/T sensor; B: Testbed for soil-screw interaction investigation at TalTech; C: measurement setup axis

Several experimental conditions were tested, including combinations of the following:
- Three different ground materials: dry sand, wet sand and gravel.
- Two different types of motion: free running (2DOF) and pulling on a bungee cord.
- Four different loads (weights) on the actuator (0kg, 2.5kg, 5kg, 7.5kg).
- Six different nominal rotation speeds (10,20,30,40,50,60 RPM)
- Five replicates of each combination.

This accounts for a total of 3x2x4x6x5=720 tests. Among these tests, a few were not performed due to motor power limitations (e.g., the motor was not able to rotate the screw when on gravel, pulling on bungee, with 7.5kg) or trivial behaviour (e.g., the actuator was digging all the sand out and not moving forward when moving on wet sand with bungee and 7.5kg).

Raw Results and initial processing

An example resulting datasets are show for wet sand experiments for free running experiments and for pulling experiments with bungee cord. The interpretation of the data was done when the RPM was reached for running experiments (to avoid transient sections) and last 5 seconds to find maximum pulling forces on the bungee experiments. Raw data with selected interpretation sections are marked on figure 6:
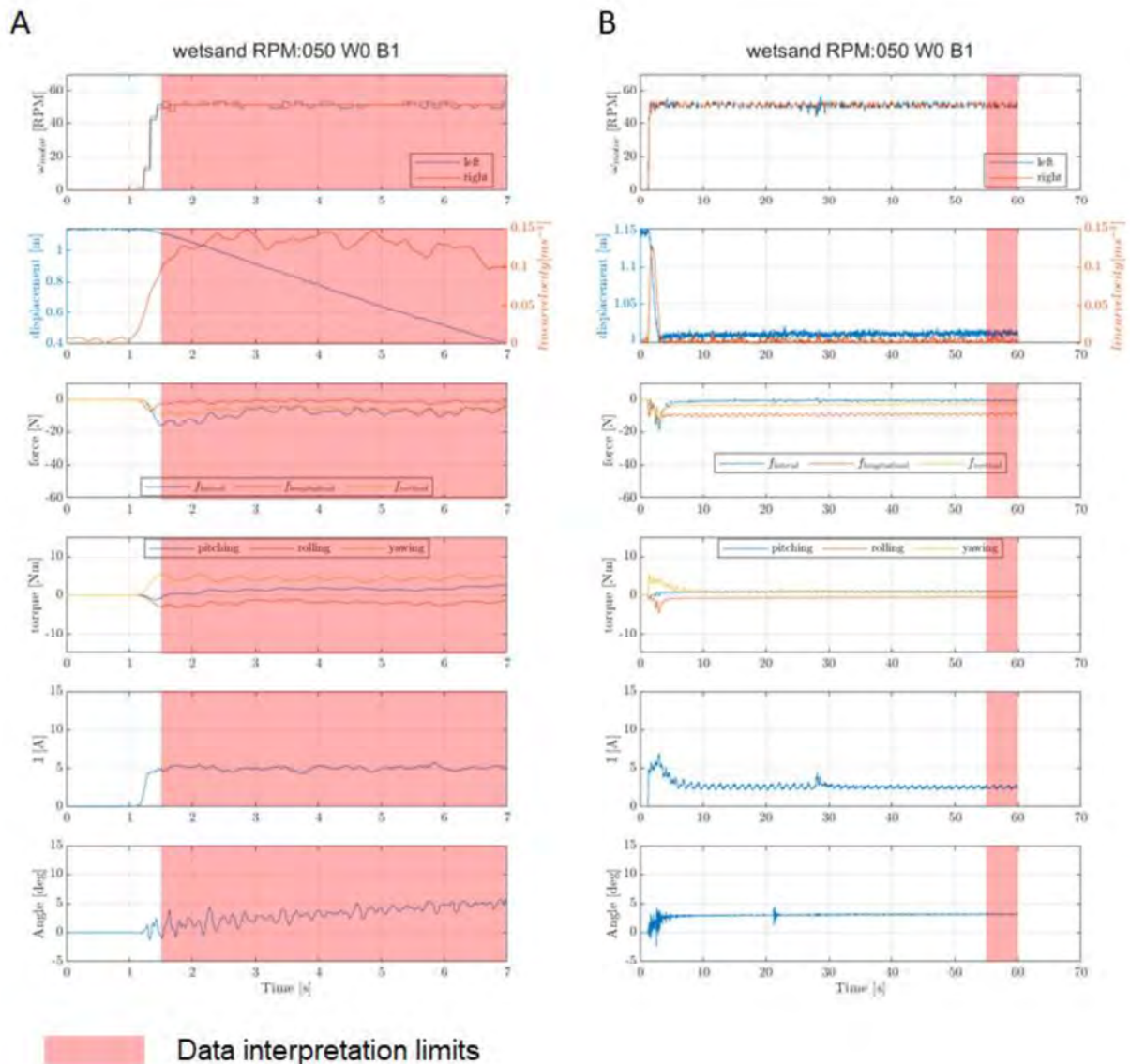
Figure 6 Raw data examples of A: Running experiment and B: bungee cord pulling tests.

The initial experimental runs were evaluated for errors visually after each run and initial matrix of results were found by looking at the mean values the replicas of each measurement combination. Standard deviation of the runs was calculated to look for inconsistency of the measurements. The relative slippage was evaluated between the slip free kinematics model and the estimated velocity from the ToF sensor. Examples of the pre-processed datasets for wet sand cases are given in figures 7 and 8 below:

ROBOMINERS-bungee-experiments-wetsand
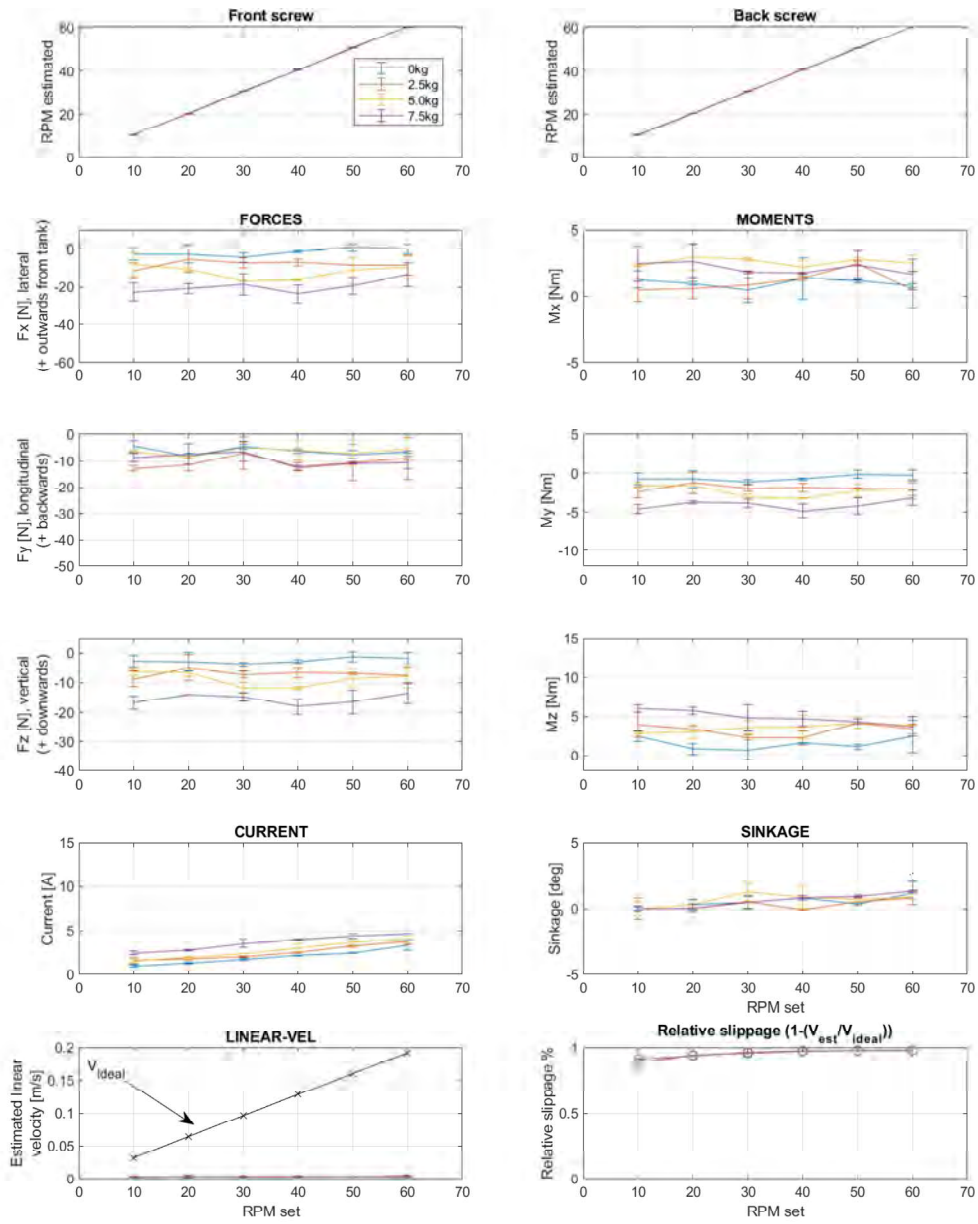
Figure 7 Pre-processed dataset from wet sand bungee experiments
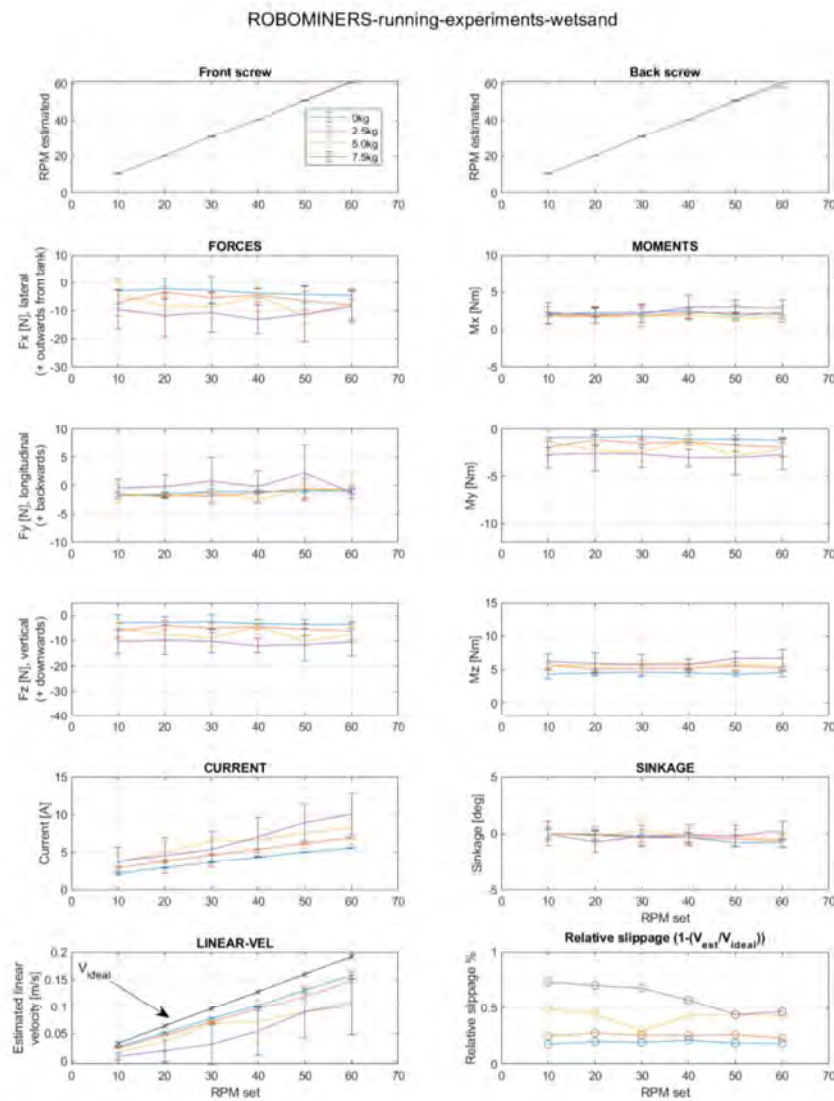
Figure 8 Pre-processed dataset from wet sand free running experiments.

All the pre-processed experimental results can be found in Appendix 1.

Data Analysis

The aim of the data analysis was to investigate the relationship between the terrain and the recorded data. Each test recording was considered as a separate input point and labelled according to the terrain it was on. The classification was done in an unsupervised manner, and resulting classes were compared to the terrain The data analysis was done separately for running and bungee experiments.
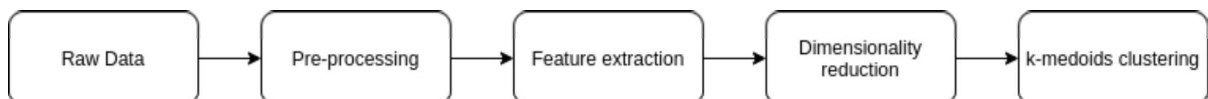
Figure 9 Soil-screw interaction data analysis steps

Figure 9 shows the workflow diagram for the data analysis. All recorded data was smoothed using local regression with weighted linear least squares and a 1st degree polynomial model. The recorded forces, torques, and current were z-score normalised and together with tilt angle data considered as input. From set input data we computed simple features, namely range, minimum and maximum of each

variable, and the mean and standard deviation of the tilt angle. The principal component analysis (PCA) was used to reduce the number of dimensions and help us visualise the data. Results of the two experimental cases are shown below:

- **Bungee experiment** - The first two principal components explain 85.5% of the variance in the data, and these were used to visualise the data. The dimensionality of the data was reduced to first 7 principal components that explain 98% of the variance. The classes were found using k-medioids clustering, with k=3 and cityblock metric to calculate the distances. The clustering was repeated 150 times to ensure the convergence and repeatability of the model. Finally, the clustered data was compared to the terrain labels, resulting in over 93% overlap. The Figure 10 shows the resulting classes using k-medioids clustering. The three classes are well separated. The misclassified points are highlighted in black.
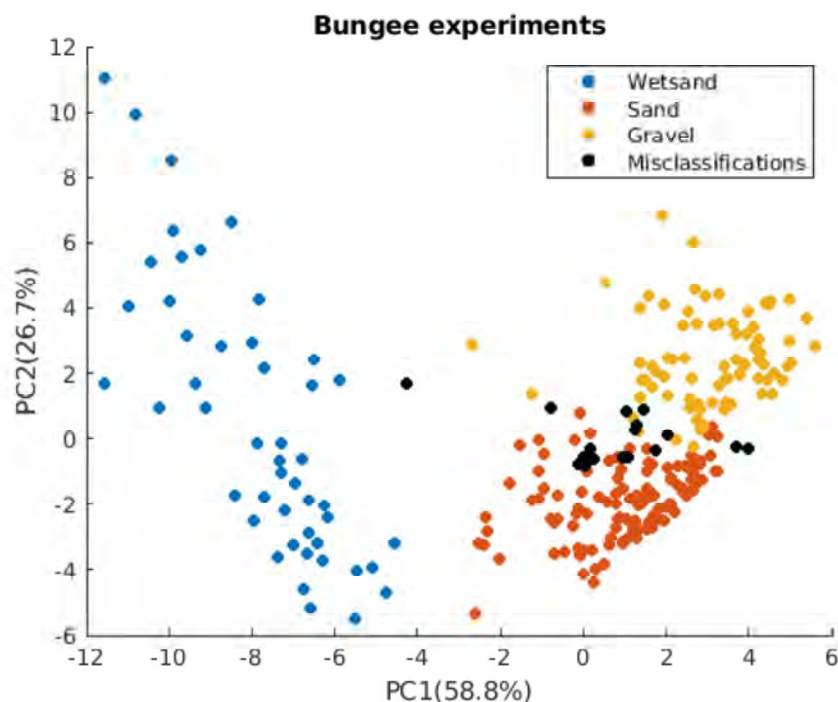
Figure 10 Classification of the bungee experiments

- **Running experiments** - For the running experiments, the first two principal components used to visualise the data explain 73% of the total variance. Similarly, to the bungee experiment, the k-medioids clustering was used, with 150 repetitions and cityblock metric. The achieved accuracy was 86.7%, slightly lower than for the bungee experiments.
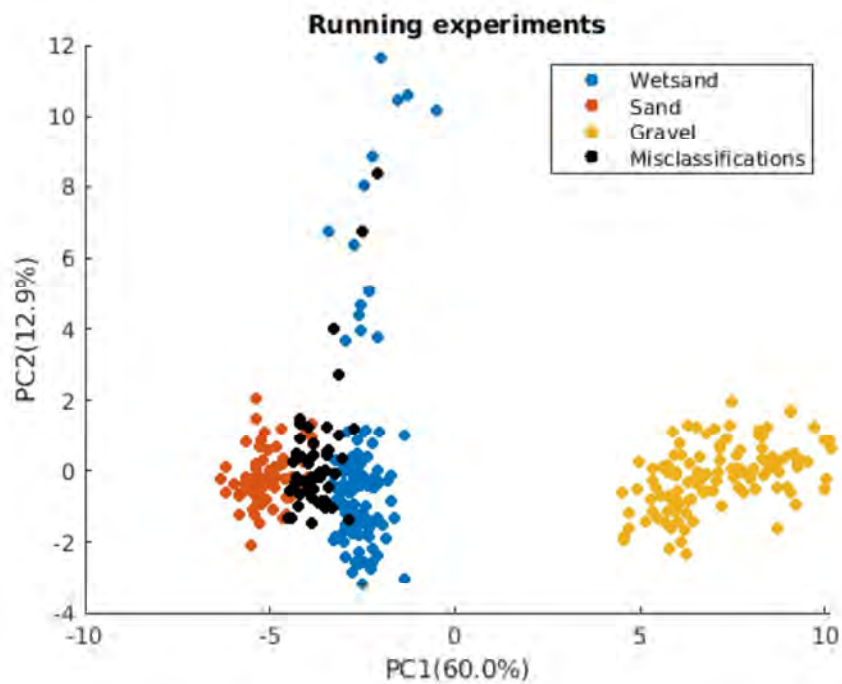
Figure 11 Classification of the running experiments

Next steps

Within the next steps of the locomotive research and development we will aim at working on following topics:

- Slippage control and odometry model improvement with soil sensing
- Improve the odometry model with other sensing modalities (e.g. touch based sensing of ground and walls) to improve accuracy of the mapping and localization
- Apply the control method on actual prototypes with several locomotion units

2.3 CONFIGURABILITY

Configurability of the ROBOMINERS system is important for improvement in locomotion capabilities, fault tolerance (e.g. how to move if one of the screw modules fails) and flexibility to adapt the robot's size and reach to a wide range of geological scenarios. The following section describes configurable alternative platform for configurability investigation developed by UPM and the experimental setup for artificial water muscle testing that will be used on the final prototype to reconfiguration of the robot's diameter and tool movement as shown in D3.2 (Aaltonen et al. 2020).

2.3.1 Platform for configurability investigation by UPM

UPM has been mainly focussed on the development of physical scale models for the purpose of studying modularity and re-configurability. Physical prototypes have been developed starting from previously developed models that have been adapted to study different configurations (Figure 12).

Figure 12 . Early prototypes of modular legged robots. Each leg is a complete robot. Left: physical prototype, right virtual prototypes. Different kinds of gaits and configurations can be created

After the consortium's decision on the final design concept of the robotic miner, UPM has been working on the development of a scaled prototype resembling the robot concept presented in D3.2 (Aaltonen et al. 2020). UPM´s platform (Figure 14,

Table 2) is based on a highly configurable heterogeneous modular robot design, with self-assembly and dynamic power sharing capabilities. The modules are equipped with technical solutions that would allow self-assembling. Concretely, the connection between modules is carried out by means of a telescopic soft robotic arm (which is under patenting), that incorporates at its end an active port that attaches to the rear plate of the neighbouring module.
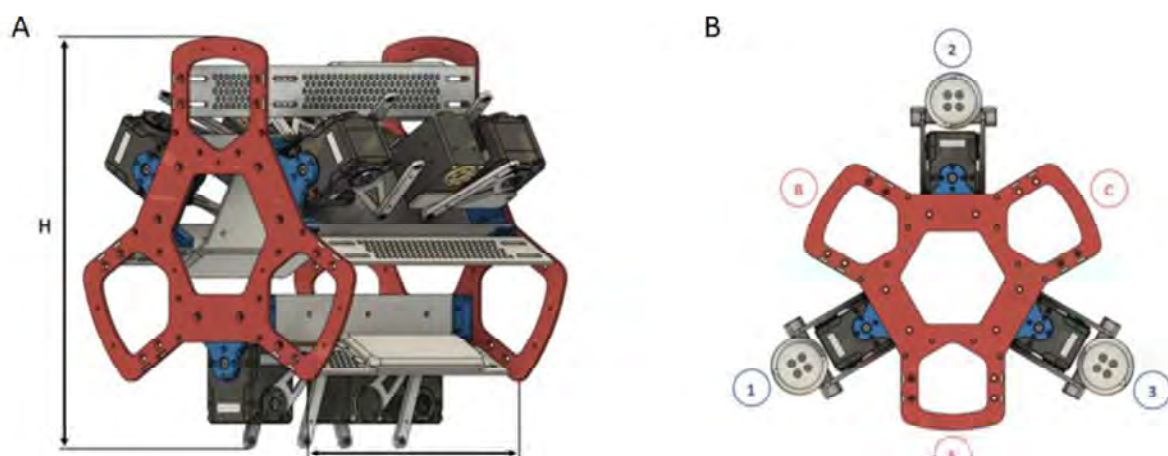
Figure 13 A: UPM´s Platform main dimensions. B: Robot Module compartments and submodule assembly ports

Table 2 UPM´s module main dimensions

Variable	Value	Units
Robot Height (H)	25.33	cm
Robot Length (L)	17.60	cm
Robot Weight (W)	1.87	kg

The individual modules of the robot (see Figure 13 B) are composed by a main structure, with three compartments (A,B,C) where the electronic components are located, and three submodule assembly ports (1,2,3) that can be equipped with different interchangeable locomotion means (e.g. screws, legs, wheels...), as shown in Figure 14.
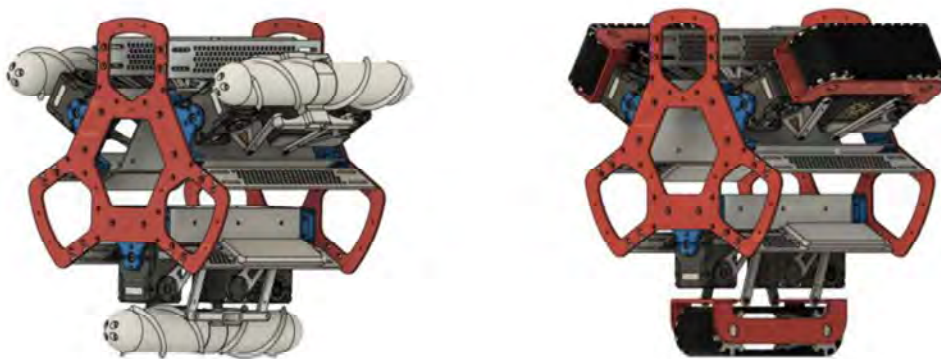
Figure 14 Different locomotion configurations of UPM´s scaled prototype. Left: screw locomotion; right: tracks

It is worth noting that the connection system for screws/tracks is based on parallel 4-DoF actuated mechanism that can also be used as a leg (see Figure 15).
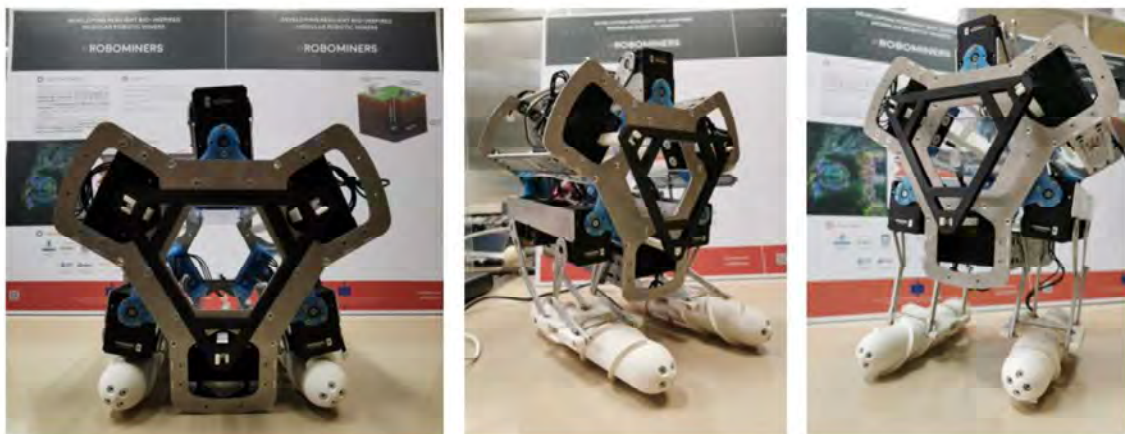
Figure 15 PM´s Platform locomotion system

Moreover, UPM has been designing a dedicated control electronics board for the prototype. Following in-house know how and adjusting to the new requirements for simplicity and space optimization, a new electronic board has been developed that includes:
- Entry protections.
- Motors and external ports current sensors.
- External charging system with intensity limiter.
- Short circuits protection system with a thermal switch.

- Stage of step-down converters. (12V, 5V, 3.3V).
- Communications hardware: TTL, I2C and CAN.
- WIFI and BT included in the microcontroller.

The current version of the PCB board released is shown in the Figure 16 .
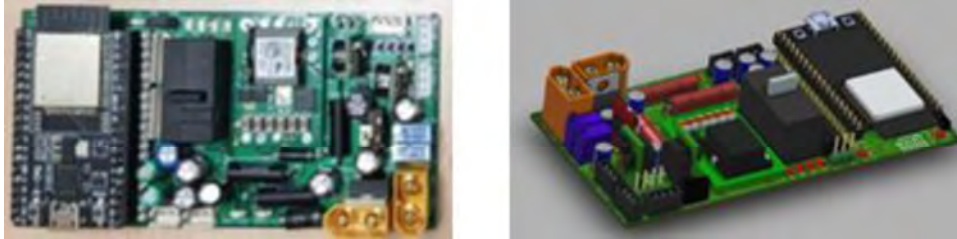
Figure 16 UPM's platform PCB design

2.3.2 Water Hydraulic Artificial Muscles by Tampere

In order to reconfigure the leg/screw mechanisms and to manipulate the drilling head, water-powered Hydraulic Artificial Muscles (HAM). This type of actuators has a very simple architecture (elastomer bladder surrounded by an inextensible braided mesh) with no moving parts that should resist the harsh mining conditions.

A testing rig has been built at Tampere University with the objective of testing HAMs in similar environmental conditions (pressure levels, temperature levels and external medium) to the ones the final ROBOMINERS prototype (reference to D3.2) will experience. The expected outcomes of the tests are to gather data regarding the static force-displacement outputs and the dynamic behaviour of several HAMs whose length will vary.

Experimental setup:

The test rig (Figure 17) consists of a double-acting hydraulic cylinder, hard mounted to a steel frame, powered by an oil hydraulic power pack and controlled by the means of a PI-controlled servo-valve with position feedback. The muscle to be tested is fixed at one end of the cylinder and hard mounted to the steel frame at its other end. A separate water hydraulic circuit is used to set the pressure level inside the muscle to the desired value. Beckhoff's Twincat3 automation software is used to automate the rig and measure the data.
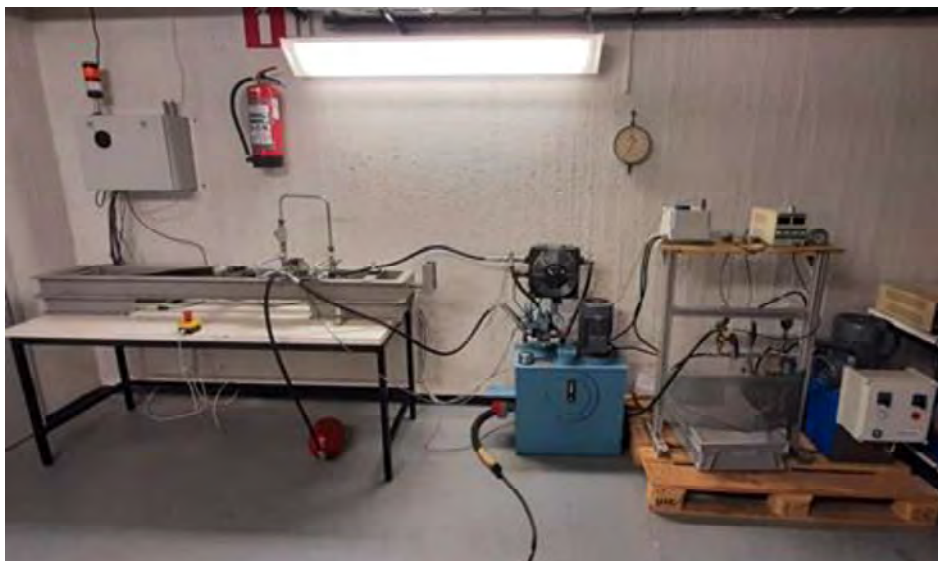
Figure 17 Test rig (left), oil power pack (middle) and water power pack (right)

The test rig is equipped with the following measurement sensors:

- **Force sensor**: TECSIS F2301 (50kN rated) to measure the muscle's reaction force output

- **Position sensor**: WAYCON LAS-T-500-A; optical sensor to measure the cylinder's displacement,
- Pressure sensors:
  o 3x TRAFAG NAH8253.74; to measure the oil pump and both cylinder's chambers' pressures
  o TRAFAG NAT8251.80; to measure the muscle's pressure level

Static tests procedure:

Once the HAM is mounted onto the test rig at one end and the cylinder at the other end (see Figure 18), the pressure level within the HAM is set to the desired test value. The muscle is then pressurised but kept at its nominal length, hence exerting its maximum force output. Then the cylinder is moved at constant speed so that the muscle's full stroke is achieved. The cylinder is finally returned to its original position.
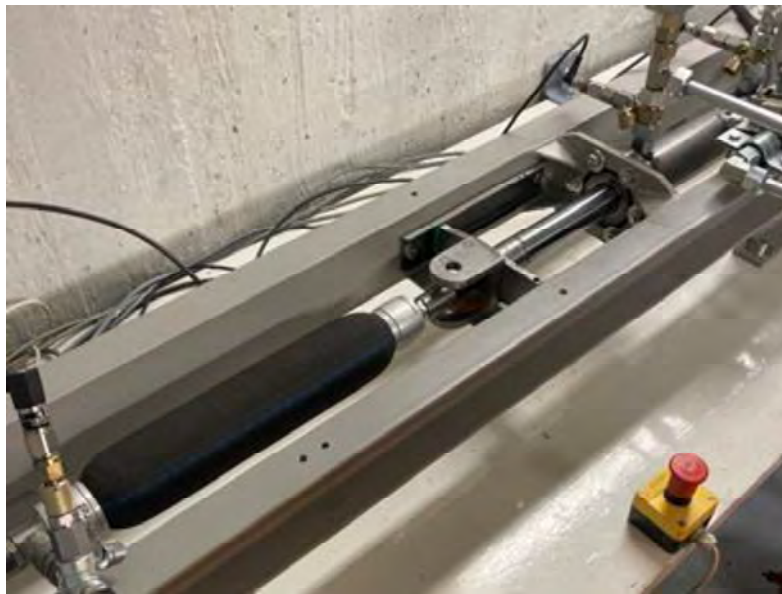
Figure 18 Ongoing static HAM test: full stroke achieved

Next steps:

The static tests are currently ongoing at Tampere University. Gathered data will be used to derive an analytical or numerical static force model that will be used for low-level control of the actuation. The test rig will also be upgraded in order to achieve testing at different external temperature levels and external media surrounding the HAM. Dynamic tests requiring an upgrade of the existing oil power pack will be conducted.

2.4   SOIL YIELD POINT SENSING AT TALTECH

To investigate soil behaviour under robot loading, a first principal study is ongoing at TalTech within a PhD project that is following one of the proposed ideas for locomotion in D1.2 (Ristolainen, Kruusmaa, and Godon 2020) The aim of this study is two-fold. The first aim is to investigate soil behaviour under different loading conditions to design a model accordingly. The second aim will be to investigate force control (or impulse control) that enable to maximize impulse while reducing displacement (hence reducing soil deformations and energy losses). The further goal is to develop an adaptive robotic leg for locomotion on low-yield soils.

For the principal study a test rig was built which consists of a linear actuator with position feedback, and a force sensor. The experiments are proceeding as follow: the test rig is introduced in the ground until a defined position, at a defined speed, and the vertical force is recorded. The experimental setup can be seen on Figure 19. On top of looking for control options for reducing energy losses and increasing impulse, some mechanical solutions are also investigated: using different foot compliance and mechanical design. Early feet samples can be seen on Figure 20.
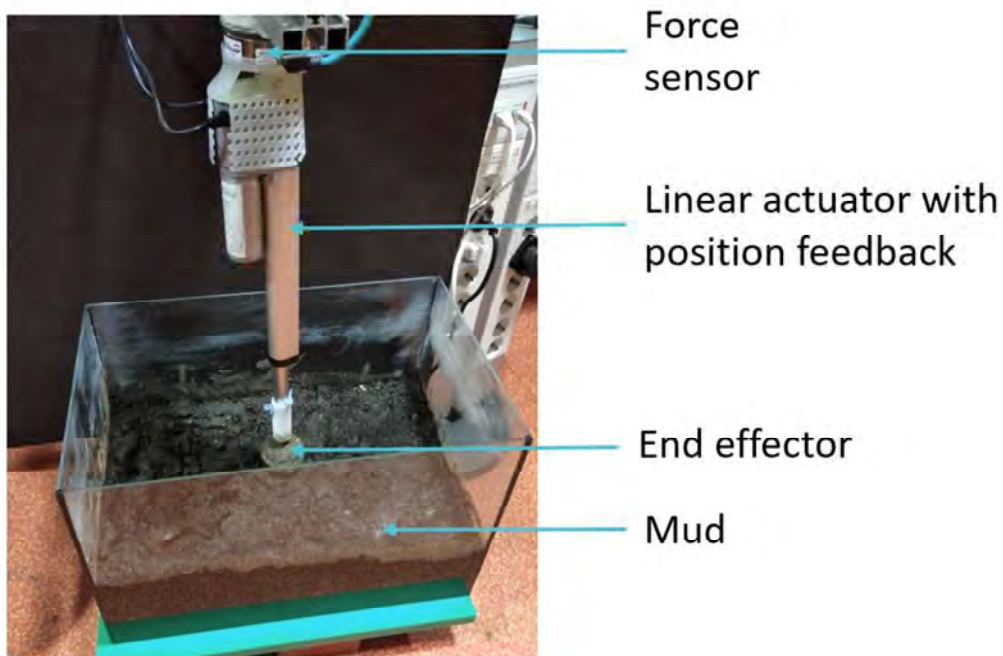
Figure 19 Soil yield-point measurement setup

Figure 20 Early feet samples with varying stiffness

Typical curves obtained for one test run can be seen on Figure 21. The impulse (force·time) can be observed in green, which is a quantity we want to maximize for locomotion. Work (deformation of the material) is marked in red, which the is dissipated energy we want to minimize.
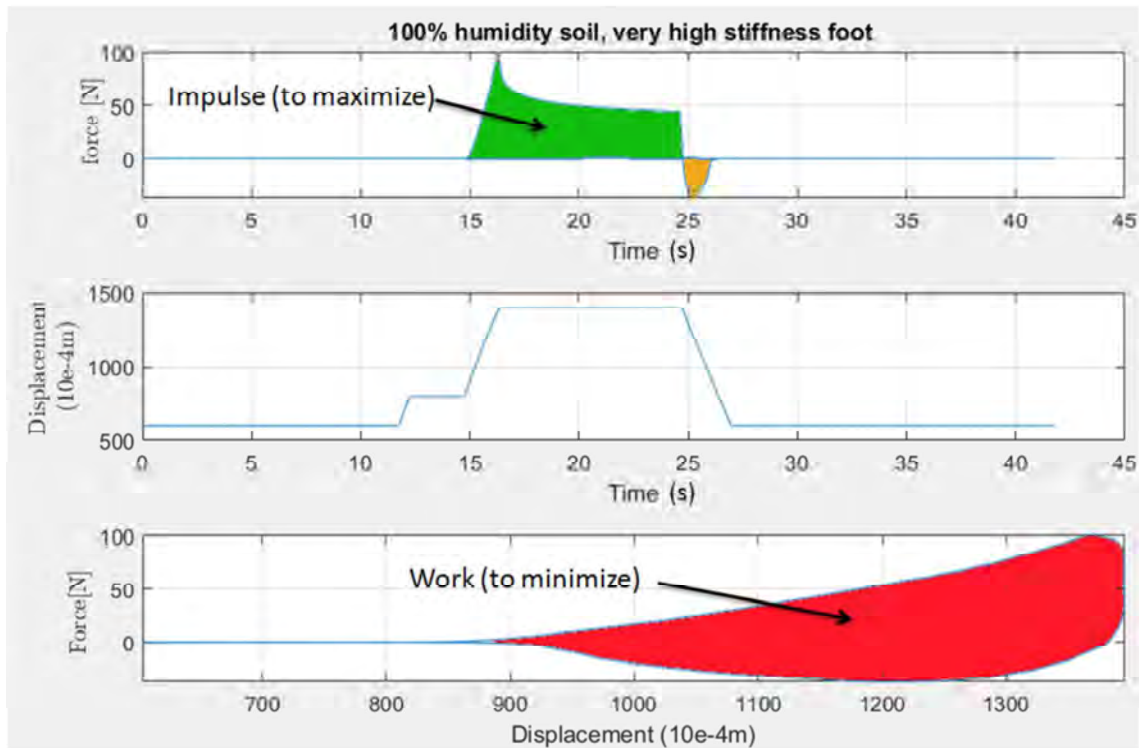
Figure 21 Sample experimental run

Within the next steps of this study control strategies and mechanical design improving the ratio impulse/work will be investigated.

3   SENSING

In this paragraph, we present early experimental perception techniques that have been tested for mapping the mining environment listed within D6.1 (Burlet et al. 2020). This section shows the progress for blind mapping with touch sensors, LIBS spectrometry, integrated IMU experimentation for usage with screw locomotion and the work done for making the sensors fail safe for high pressure scenarios.

3.1   WHISKER BASED BLIND MAPPING BY TALTECH

Several animal species – both terrestrial and marine – use whiskers (vibrissae) as a sensing mechanism for navigation in the near-field environment (Solomon and Hartmann 2006). With the TalTech test platform we explore the possibility of this bio-inspired feature by implementing an array of stems sticking out downwards and sideways from the robot body which deflect upon contact with objects. The information collected by means of these whiskers is intended to help the robot in navigating around obstacles and additionally serves as a source for localization and mapping. Using 32 whiskers on the prototype, we have experimentally explored the ability to sense and identify features on the ground below the robot and proven in simulation that the collected information can be used as input to a SLAM (simultaneous localization and mapping) algorithm to improve the odometry estimation and create a map. Tests with 64 sensors (32 pointing downwards and 32 sideways all around the robot) have also been carried out and are demonstrated in this section.

3.1.1   Experimental setup

Description of the test platform

In this experimental setup we assembled a test platform using 2 screw modules along with 64 whisker sensors (32 horizontally oriented around the side of the robot and 32 vertically oriented underneath the robot). The vertical whiskers were equipped with 150mm long stems (not touching the ground in rested state) and the horizontal ones with 200mm long stems.
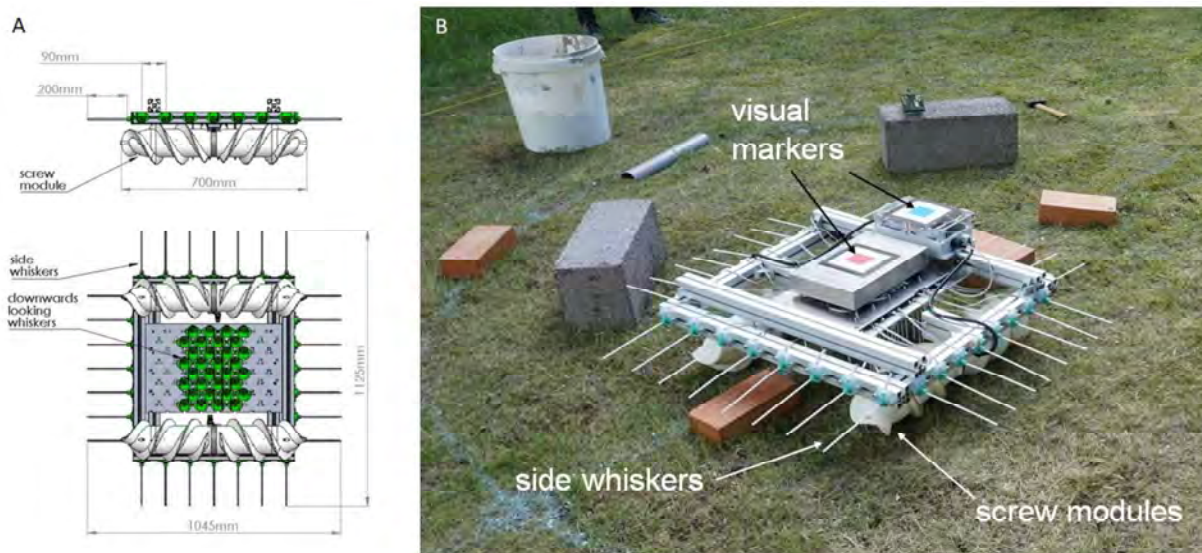
Figure 22 Experimental platform for blind mapping study. A: Platform dimensions and placement of whisker sensors. B: Test platform in lab scale mapping testing

The test-platform was equipped with following sensors:
- **IMU** – one BNO080 (by Bosch) is installed in the centre of the platform (middle box in the figure above) and one into the front of the platform (box with blue marker in the figure above), recording angular velocity and angular position around the 3 primary axes.
- **Whiskers** – custom made tactile sensors based on 3D hall sensor and compliant joint material (see longer description below)

- **Temperature** – MCP9808 (by Microchip Technology Inc) I^2C precision temperature sensor (inside the blue box, see figure XXX).
- **Current/power** - INA219 (by Texas Instruments) current shunt and voltage monitor for each motor in the platform's actuators.

Whisker functional overview

A whisker is a device that can be used to sense the presence of objects through physical touch. In the case of the ROBOMINERS prototype, it consists of a Hall sensor and a mast with a magnet attached to the end closer to the sensor. The mast is held in place by a compliant joint made of silicone rubber. Any deflection of the mast leads to a deflection of the magnet above the sensor, which senses the strength of the magnetic field in 3 dimensions. The sensor computes the magnet's deflection and transmits this information as Cartesian or spherical coordinates to the microcontroller or computer. As the compliant joint is more flexible than the mast, we assume that the deflection of the magnet corresponds to a deflection of the whisker and therefore to a deflection of the mast's outer end point.

Figure 23 shows the physical design of a single whisker sensor unit. Each of these is mounted individually on the robot platform. This allows for ease of reconfiguration during various test scenarios. The housing is partially 3D-printed and partially cast from silicone. The silicone provides the masts the required ability to deflect and bounce back to the resting position.
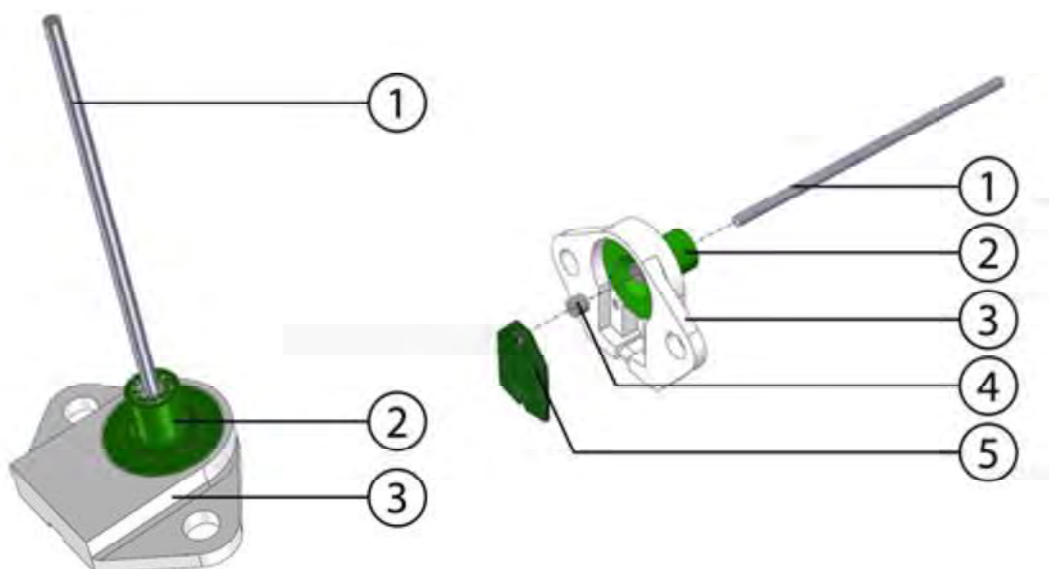
Figure 23 Whisker unit physical design. 1: mast (nylon), 2: compliant joint (silicone rubber), 3: housing (photopolymer), 4: neodymium magnet, 5: PCB holding the sensor chip.

Description of the data acquisition

An A64-Olinuxino computer, running ROS2 Foxy on Ubuntu 20.04 was used to interface all 64 whisker sensors and one BNO080 IMU. All other devices of the robot were interfaced by another A64-Olinuxino computer. ROS2 nodes have been written for interfacing each type of device. The experiments were semi-automated using launch files. Three computers running ROS2 participate in the experiments. All computers are connected to the same network and are configured to be able to access each other's ROS topics.

Experimental sets

The experiments with the test platform were performed in two sets. The first experiments were conducted in a controlled environment on a flat grass surface and the second, limited set of experiments took place in a closed mine at Ülgase, Estonia, which is an abandoned phosphorite mine.

Controlled environment

4 scenarios were investigated within the controlled experimental set. The path of each following scenario was longer and included more rotations. The scenarios followed similar tracks that were studied prior within a simulated experiment (see section 4.1). The first controlled environment experiments were conducted on flat grass surface with dimensions of 6 by 6 m. The scenarios 1 to 4 are shown in the figures below:
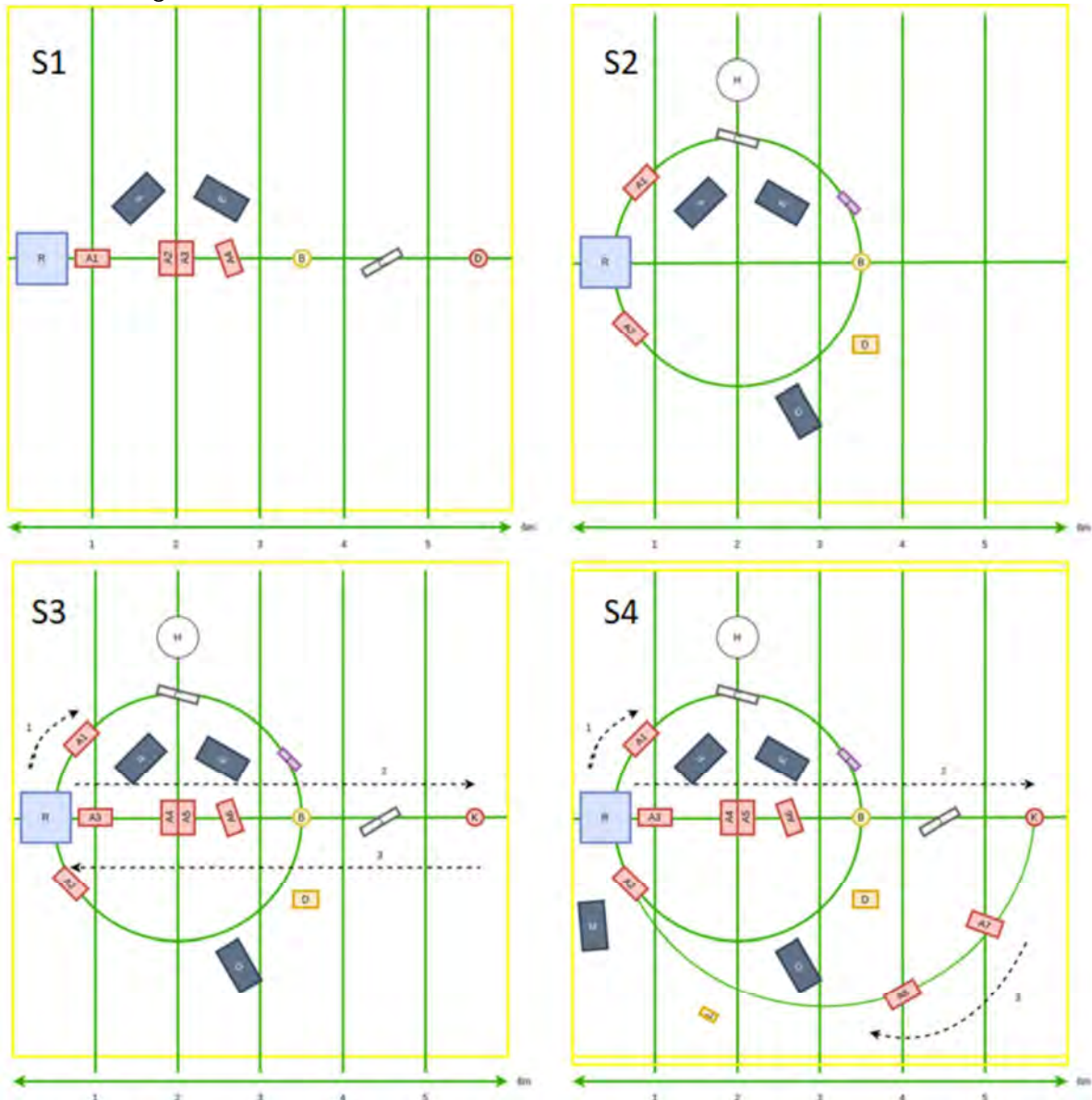
Figure 24 Controlled environment test scenarios 1 to 4

A set of artificial objects were placed to the test ground for mapping purposes both with the side whiskers and with the downfacing whiskers (referenced to Figure 24):

- **Low objects**: 6 x bricks (A1-A8), hemisphere (B), long thin half cylinder (C), hammer (I), thicker half cylinder (J), cylinder weight (K)
- **High objects**: big bricks (E), (F), (G), (M) bucket (H), double vertical bricks (D), single vertical brick (L)

The robot trajectories in the scenarios 1 to 4 were following:

- **SC1**: Straight line (approx. 5m) -> turn around on the spot (180 degrees) -> Straight line (approx. 5m)
- **SC2**: 1 x the circle (r=1.5m), clockwise

- **SC3**: 1 x the circle (r=1.5m) followed by the straight line. (Order shown in order 1,2,3)
- **SC4**: 1 x the circle (r=1.5m) followed by the straight line and back following half circle (r=2.5m) (Order shown in order 1,2,3)

The robot's location within the above-mentioned scenarios was tracked from above with a GoPro Hero 5 action camera with a time-lapse interval of 0.5s. The robot track was later reconstructed using two markers on the test platform (Figure 22) for x-y coordinates using the red marker and heading using the blue and red marker configuration. The tracking was done with Kinovea (https://www.kinovea.org/) software. For additional simulation purposes and mapping the artificial object's locations, a 3D map of the test ground was reconstructed using Agisoft Metashape Professional software and a mirrorless digital camera (Sony a6000, 16-50mm lens). A resulting map is shown below.

Figure 25 Controlled environment tests. A: reconstructed 3D view of the test ground. B: Camera based tracking of the test platform location

Mining environment

The second set of experiments are done in an old abandoned phosphorite mine at Ülgase. The goal of this experiment is to perform localization and mapping natural mining scenarios, where the whiskers are used to track the features of natural wall and floor. A 21 m long U-shaped path was chosen in the mine for testing that is shown in the reconstructed map below (Figure 26).
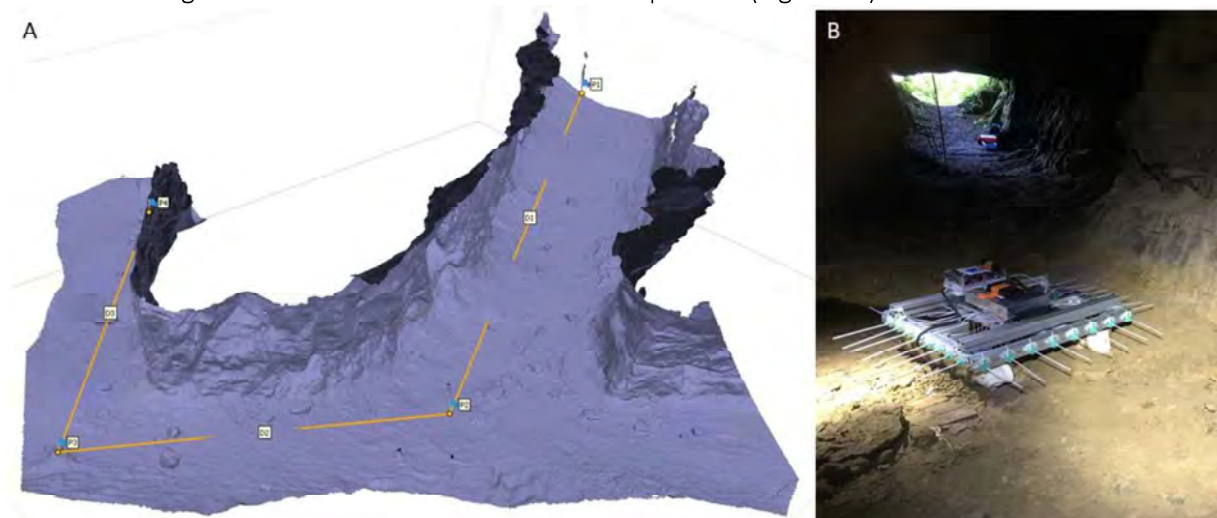
Figure 26 Experiments in an old phosphorite mine. A: Mine section 3D reconstruction and the 21m path. B: Test platform in the mine

3.1.2   Results from data acquisition in controlled environment case

This section shows the results of a preliminary processing of the data from the experiments in the controlled environment. Here are included only the vertical sensors that are positioned below the robot, between the actuators. The data pre-processing was performed on the recorded 'bag' files that were collected during experiments. The aim was to determine if the whisker sensors' data indicate the various features, without any sophisticated processing required.

The metric that was used is the absolute change of magnetic field strength, averaged for all vertical sensors. This corresponds to the average deflection of the vertical sensors, for each time instance. Example results of this can be seen in Figure 27. Cross-referencing with Figure 24, shows that each peak in average deflection corresponds to one of the features on the terrain. Additionally, the height of each peak corresponds to the volume/height of the feature it describes.
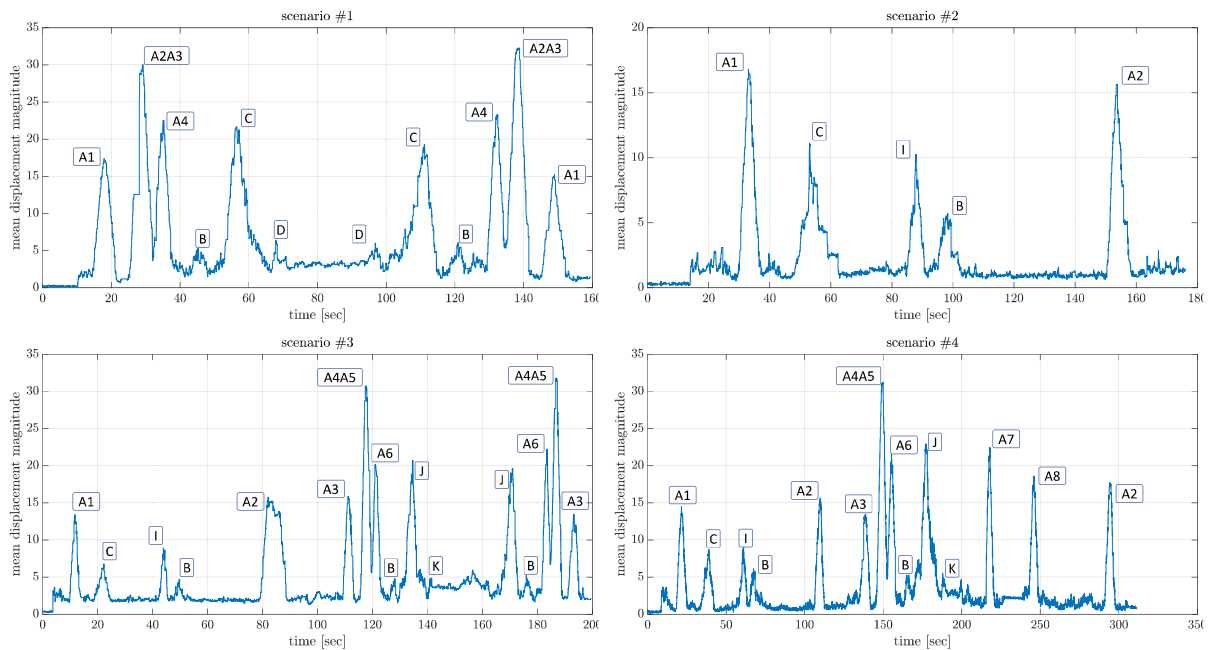
Figure 27 Preliminary results of experiments in a controlled environment

3.1.3   Next steps for blind mapping studies

Within the blind mapping study, the next set of experiments and developments will involve:
- Finishing blind mapping experiments in the natural mining environment
- Evaluation of the gathered mapping data with offline SLAM algorithm described in section 4.1
- Ruggedization of the whisker sensors for experiments in underwater and slurry scenarios
- Integration of other sensor modalities into the SLAM algorithm for selective mining purposes

3.2   IMUS AND WHEEL SENSOR CALIBRATION EXPERIMENTS BY TAMPERE

Wheel measurement system (WMS) is a MEMS inertial unit produced by Pacific Inertial Systems (Figure 28). The intended use case for it is to be mounted on a car wheel. The unit measures wheel movement and calculates estimation for speed, moved distance and current position. Drift is minimized by calculating distance based on wheel rotations and using gravity to calibrate the unit as it rotates with the wheel. The WMS is self-contained with its own processing unit and outputs data in NMEA format through a serial interface.
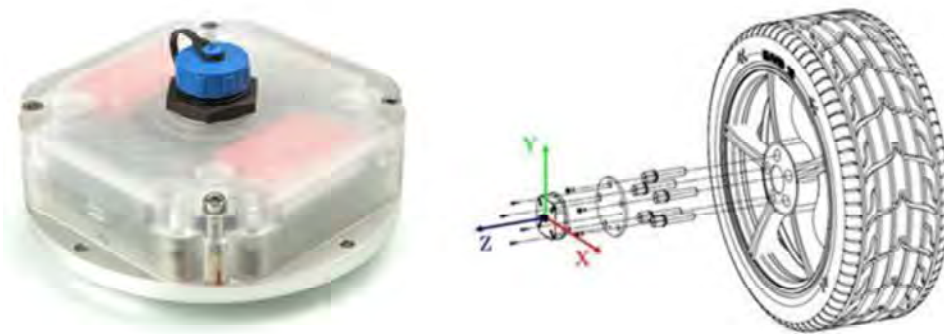
Figure 28 Wheel measurement system

To study the applicability and accuracy of the sensor on the screw locomotion module, a testbench was built to move the WMS in an axial direction emulating usage inside of a screw module (Figure 29). The testbench has a linear rail driven by a servo motor, linear movement is measured with a linear sensor. The WMS is mounted on a rotating axel, driven with a servo motor.
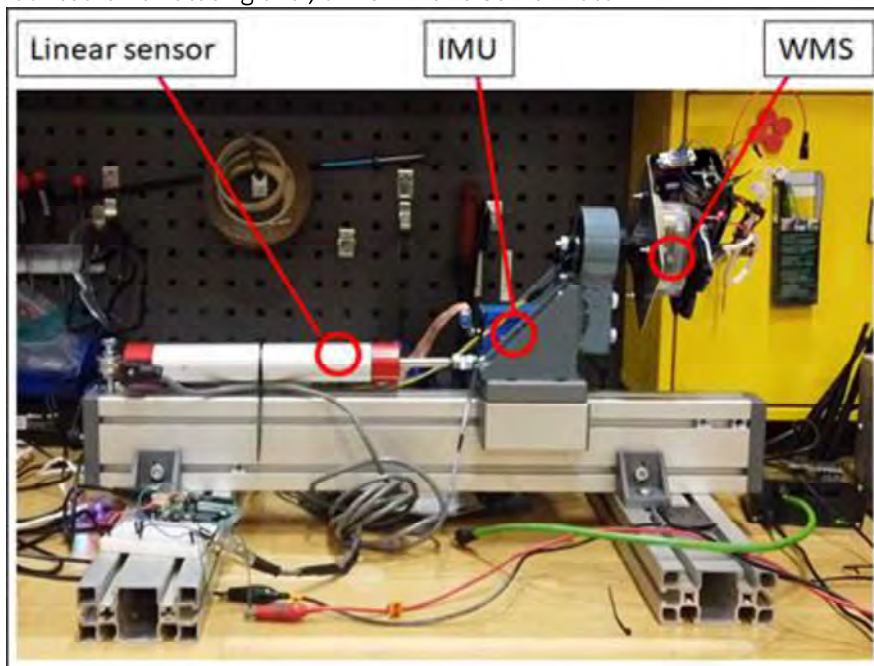
Figure 29 WMS test bench

Changing the mounting from wheel to screw and movement from radial to axial was a straightforward process. The WMS doesn't use IMU to calculate moved distance directly but through rotation, hence it doesn't matter if the actual movement direction is changed. The only thing that needed changing was tying the distance to screw pitch. The WMS outputs distance in units of rotation, when this is scaled with the screw pitch (meters/revolution) the output has the correct unit and scale. The WMS comes with a supported ROS package that was modified to tie the moved distance to screw pitch instead of wheel diameter. The modified package was also made to work in ROS2.
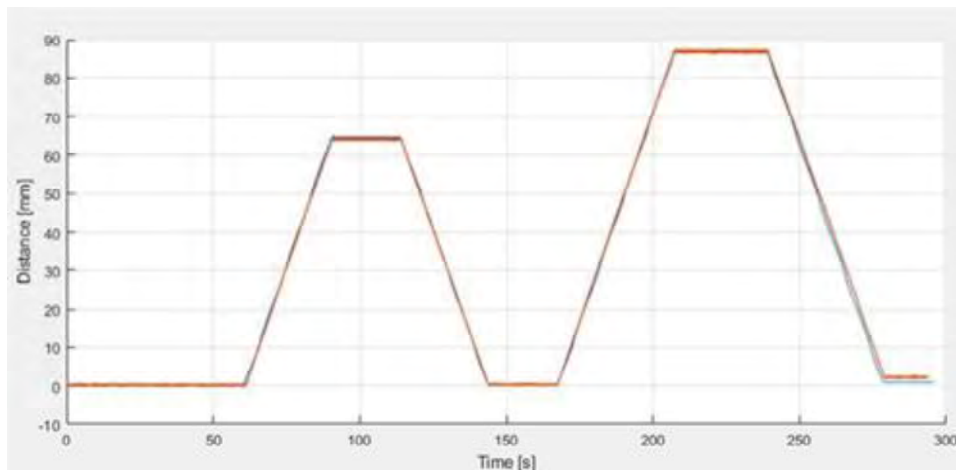
Figure 30 Moved distance comparison

Data from the test bench shows how the WMS works in near ideal condition: smooth constant movement in one direction. WMS output is compared with a linear sensor. Figure 30 shows measurements from the linear sensor laid on top of WMS x-coordinate output. The two measurements stay in sync extremely well, only a small misalignment can be seen in the final values.

One downside to the WMS is inability to sense slip. Another sensor should be used in conjunction with WMS to handle situations where the screw is slipping. The current plan is to integrate a WMS in each screw and have an accurate IMU inside the main body. A PI48 show in Figure 31 was included in the test bench, but no senor fusion was implemented at this point.

Figure 31 PI48 IMU

The experiment has shown that a WMS can be used and could be able to provide good odometry for the robot. Further tests are needed to see how the sensor behaves inside of an actual screw. More plots are included in the APPENDIX – 3 IMU test samples.

3.3 ADAPTIVE LIBS SPECTROSCOPY OPTICS USING FAST ELECTRIC TUNABLE LENSES BY RBINS

The purpose of these laboratory tests was to test and optimize an optical LIBS setup (laser-Induced Breakdown Spectroscopy) containing a varifocal optical element. We refer to deliverable 6.1 (Burlet et al. 2020) for an overview of this technique and its applicability to ROBOMINERS. In our current experiments, an electric tunable liquid lens (Figure 32) is introduced in the focusing path of the lasers (3 laser models are tested for performance comparison on solid and slurryfied ore samples). Integrating such lenses in a LIBS setup allows to change the focusing distance of the spectrometer several tens to hundred times per second, making the spectrometer much more efficient in an environment where the precise position of surface to analyse is unknown or changes very quickly (like in a turbulent slurry flow). A no current LIBS spectrometer uses this technology, a first feasibility study in the laboratory is needed to recommend and integrate this solution for the demonstration prototype.
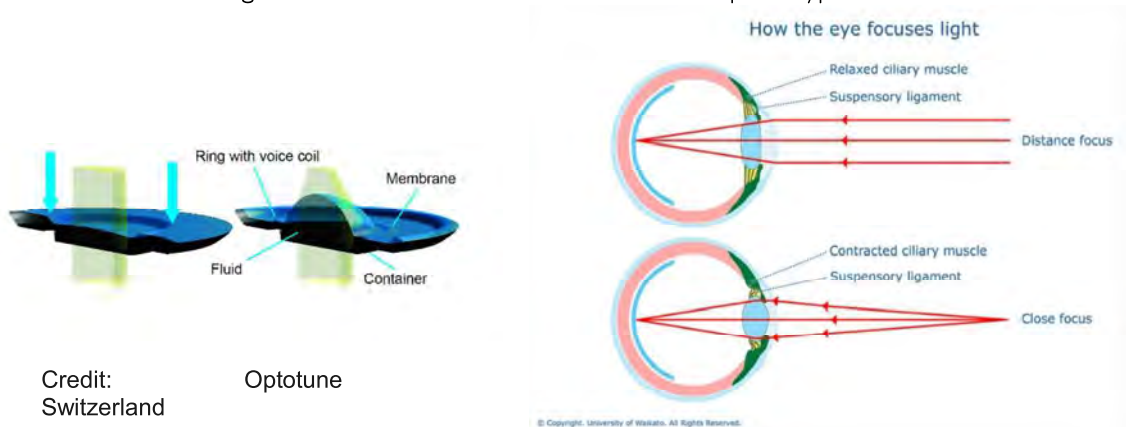

Credit: Optotune
Switzerland

Figure 32 (left) the working principle of Optotune's electrical lenses. The only movement is a ring that pushes down on the me membrane in the outer part of the lens with increasing current, thus pumping the liquid into the centre of the lens. This is analogue to the ciliary muscle contraction of the crystalline lens in a human eye (right).

Experimental set up

3 laboratory optical setups (Figure 33) were built to test a selection of pulsed laser in conjunction with tunable liquid lenses in coaxial collection configuration (Figure 34). The preliminary tests were conducted on solid ores samples (slabs and cutting) as well as on synthetic slurries. The overall objective of these experiment is to select the best instrumental setup to perform LIBS without pre-focusing the laser on the sample at a few cm distance (quasi-continuous focus on a pre-defined range). The performed analysis demonstrated the efficiency of the setup to detect major, minor and some traces elements in test materials (calcite, granite, iron and Pb-Zn ores). The major challenge still remaining is the improvement of the transmission characteristics of the liquid lens in the deep UV range, a very important spectral region for LIBS emissions. New custom-made optics are being manufactured by the Optotune company for that purpose and will be tested in 2021.

A detailed report on the results of these experiments and their proposed implementation in ROBOMINERS will be done in deliverable 6.3.
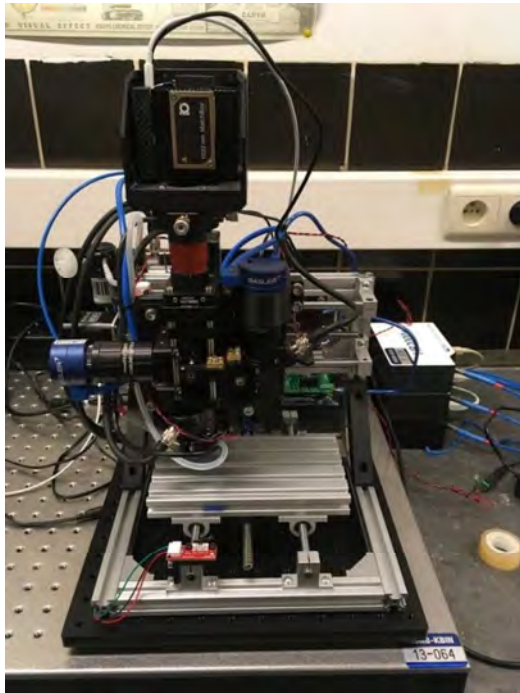
Figure 33 overview of the LIBS instrumental setup tested for ROBOMINERS. Top left: early demonstration platform for solid samples based on a microchip laser (1030nm - 100μJ/2kHz). Top right: fiber-laser based prototype (1064nm - 1mJ/20KHZ). Bottom left: slurry LIBS spectrometer, based on a DPSS laser (1064nm - 50mJ 20Hz). Bottom right: plasma spark on a slurry sample.
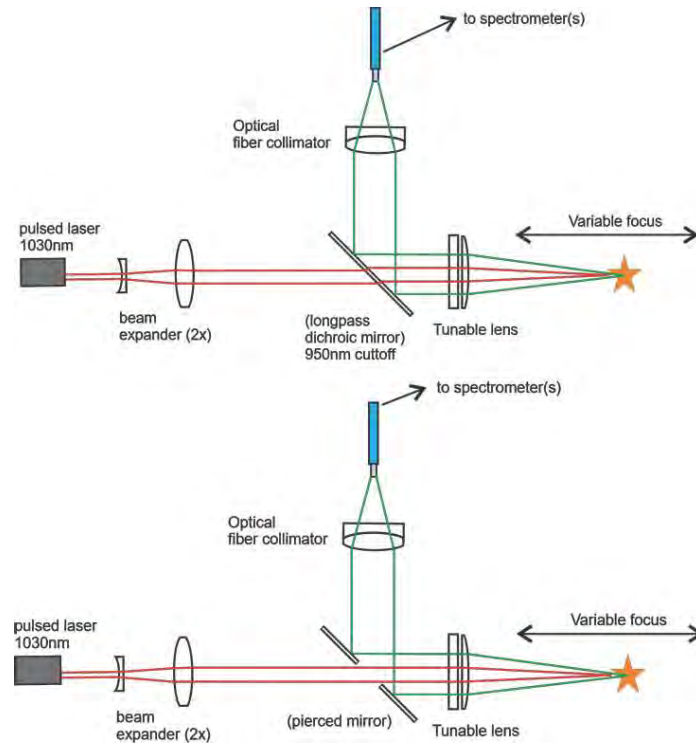
Figure 34 The two main tested co-axial optical configurations for the LIBS spectrometer (top) dichroic mirror vs (bottom) pierced mirror- to optimize UV collection toward the spectrometer

Data acquisition

Laboratory LIBS spectra are collected using a set of Avantes CMOS Czerny-Turner benchtop spectrometers (avaspec-uls4096cl-evo) with a 0.07-0.11nm resolution from 195 to 570nm. Other spectrometers have also been tested for possible integration in the ROBOMINERS prototype (Ocean Optics HR2000 and Ibsen Freedom spectrometer).

A purpose build software has been developed to test the three setups with the various spectrometers (Figure 35). The software is developed in Python 3.8 and connects all hardware components (laser, spectrometer(s), tunable lens, sample stage and micro-camera's). Basic spectral processing (peak identification and integration is done using Python's SciPy library functions.

Figure 35 Laboratory acquisition software made for ROBOMINERS LIBS experiments. A typical LIBS spectrum is visible on the left (lead sulphide)

Next steps

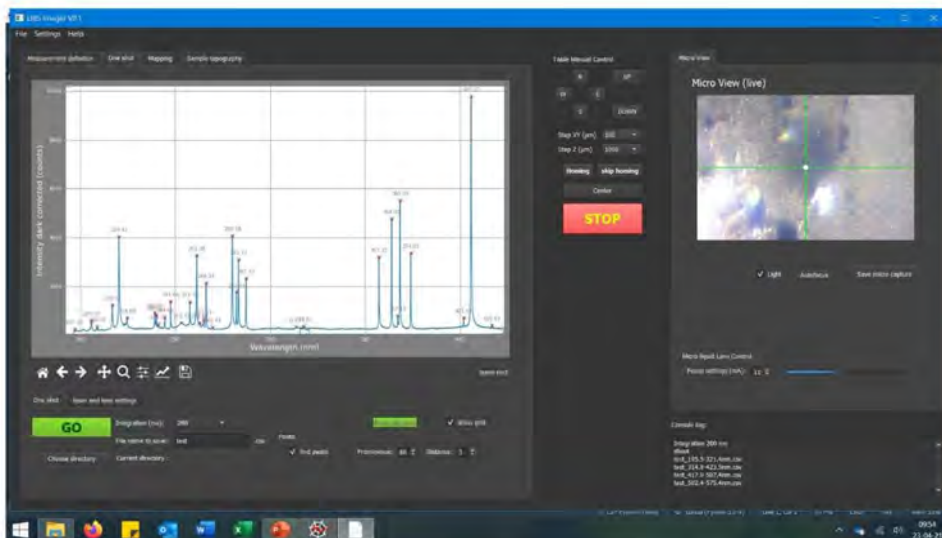The next steps for the laboratory experiment on LIBS spectroscopy will be pressurized slurry testing in a sealed steel container (see Figure 36). The experiment will use an argon bubble dispenser to create the free space needed for the laser induced plasma expansion, this gas inlet will operate in synchronization with the laser output and the tunable lens. This setup will be tested and the KUTEC partner facilities on a full-size mining slurry circulation system at around 10 bars pressure (Figure 36).
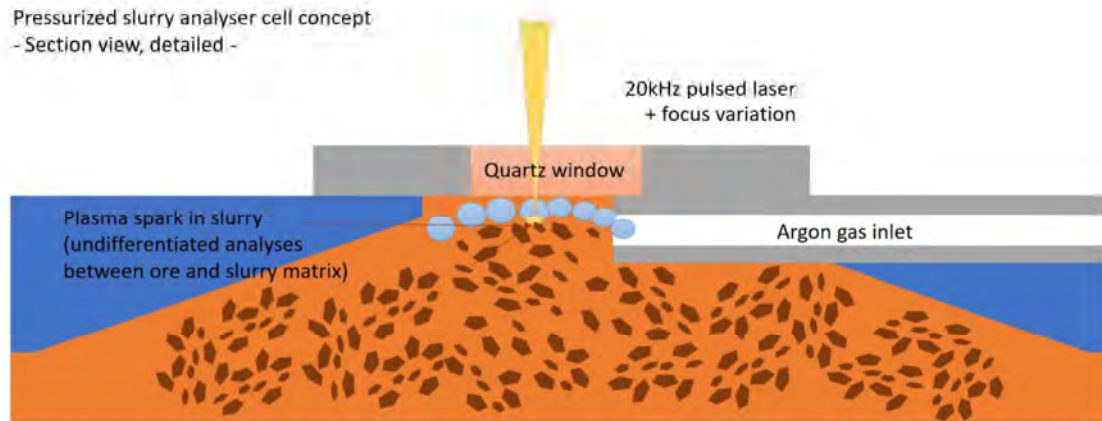
Figure 36 (top) conceptual schema of the LIBS slurry analyser test setup. (bottom) Slurry circulation device at the KUTEC facilities.

3.4   CONDUCTIVE WHISKERS BY RBINS

The implementation of the electrodes dedicated to the geophysics with the whisker are investigated to determine if the joint set up will be helpful in the selective mining and mapping process.

Experimental set up

In the current set up electrodes INOX of 4mm of diameters and 200mm length are inserted in the compliant joint in silicone of the whisker (Figure 37). The new electro-whisker is then positioned on a 3D printed structure that will allow to move the electro-whisker in the preferable position. The electrodes are then connected through jumpers to the ERT cables linked to the resistivity meter (Terrameter LS2). The equipment is powered by an external gel lead battery (12V, 90Amp/H).

Figure 37 Current set up of the electro-whisker

This first initial set up (Figure 38) is currently being expanded: the rock samples will be hosted in a box 1x1m overlayed by a grid where several electrodes array can be deployed and tested. The size and the displacement of the electro-whisker and the thickness of the used samples, that can reach 35-40cm, will be in line with the scale of the robot-miner prototype.
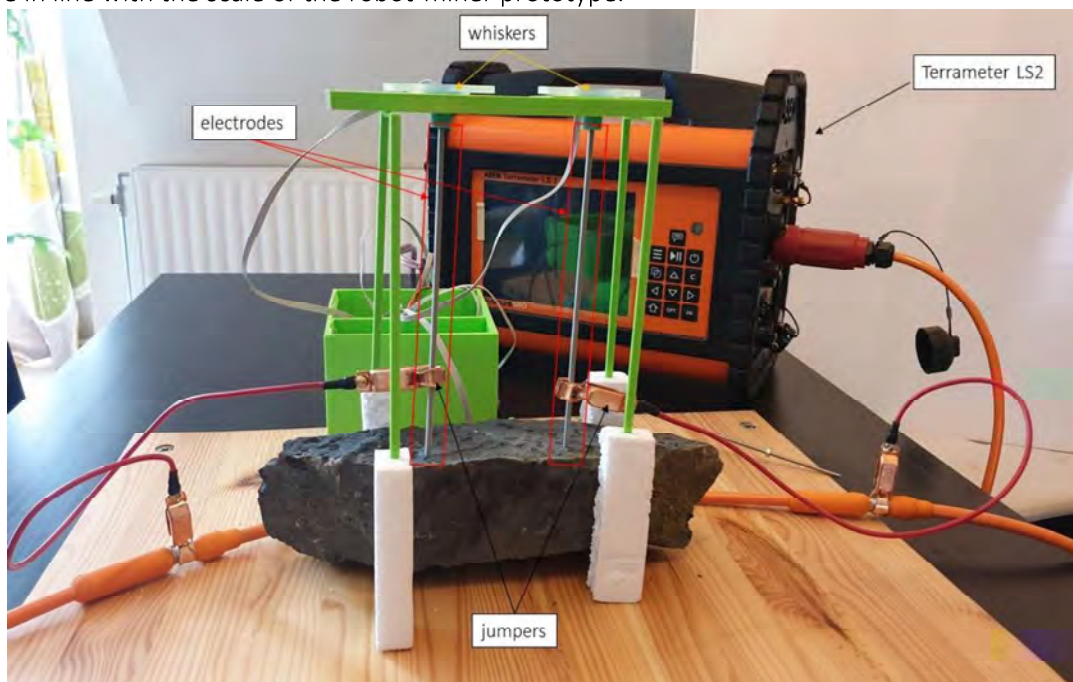
Figure 38 Initial set up for the electro-whisker test

Data acquisition
MobaXterm is used to control remotely the Terrameter and consequently the data acquisition. Different protocols are put in place according to the number of electrodes used. A processing computer running Res2Dinv and Res3Dinv is then used to elaborate the acquired data.

Next steps
The next set of experiments and developments will involve:
• Extension of the laboratory set up
• Construction of a holding structure for the electrodes (according to the robot-miner prototype design) for field test
• Test in a controlled environment and in a mine environment (dry and wet condition)
• Integration with the whiskers functionalities
• Evaluation for the integration of the sensors in the SLAM algorithm

3.5 PRESSURE TESTING OF SENSOR ELECTRONICS BY TAMPERE

ROBOMINERS project develops technology for mining in water-filled mines down to 5 km. It is roughly equal to the pressure of 500 bar or 50 MPa. Protecting the whole system from pressure is complicated and expensive. It is possible to prepare for the stress by installing the desired equipment into the pressure chamber. Said chamber keeps the pressure inside close to the standard atmosphere and the outside pressure outside, respectively. To perform the task satisfactorily, it must withstand the forces applied to it without compromising the functionality of the equipment. In a mobile device, the increase in mass, possibly due to the protective shell, changes its dynamics. It also inevitably increases the external dimensions of the device to be protected. (Hakonen 2021).

Some of these disadvantages can be prevented by protecting the components in smaller subsystems. The caveat is that standalone subsystems are not useful without interactions with other subsystems, which creates the need to guide electrical signals and mechanical movements through the pressure hull. It is possible to use connectors and penetrators for the task, further increasing the dimensions and weight (Hakonen 2021).

Data published about pressure tolerant electronics does not cover every component in detail. Comprehensive information about the subject is not publicly available, and usable results are published usually only per component and not so much for a more complicated system. Still, manufacturers are selling pressure tolerant electronic equipment working under tens of megapascals pressure. It implies that selected standard components can withstand hydrostatic pressure more than what they are designed for (Hakonen 2021).

Autonomous system is dependant of computational resources. Having said resources available at the edge of the system decrease complexity and amount of cabling. Test system was constructed to find out if commercial off-the-shelf parts can be used in the project. Setup is shown in Figure 39.
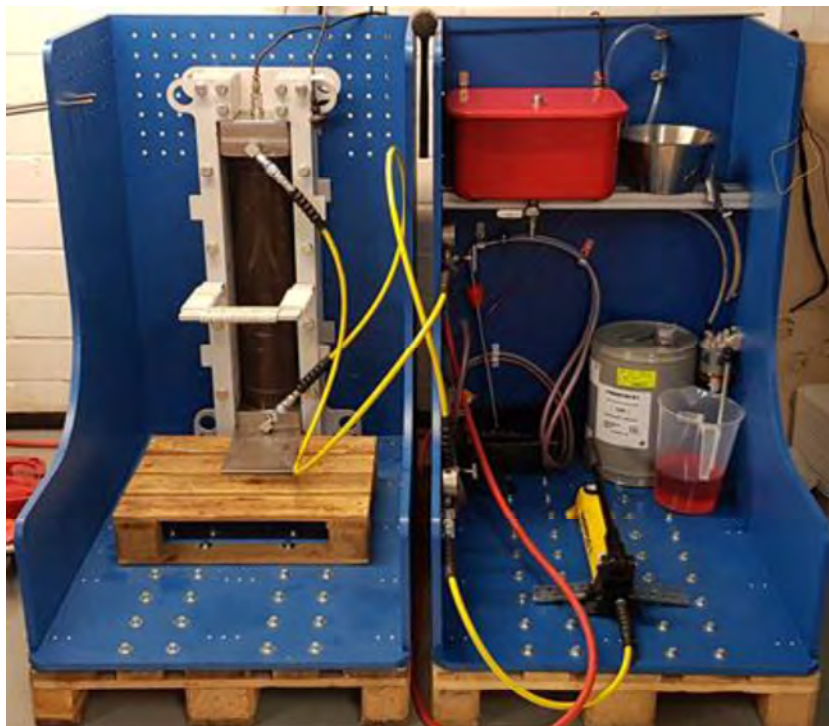

Figure 39 Pressure test setup for electronics

A single-board computer (SBC from now on) from the company Olimex Ltd. was chosen for the tests. The selected model was A64-OLinuXino-1G. It is built around Allwinner A64 processor, which is a 64-bit, 4-core Cortex-A53 CPU. Board includes a gigabit Ethernet interface without extra hardware. Design files of the A64-OLinuXino-1G are published, enabling circuit debugging. Multiple revisions of the board have been published. Revision D is shown in Figure 40. It is the revision used in the tests.

Figure 40 The topside of a single-board computer A64-OLinuXino-1G

When the microprocessor boards and SBCs were pressurized, it was observed that the crystal was first to fail under pressure. After measures were taken to protect crystals, short term pressure tolerance of the board was increased significantly. It was found that a computer with multiple integrated circuits can tolerate the pressure of tens of megapascals higher than designed, with small modifications even higher. The aim was reached when a single board computer was working under the pressure of 50 MPa as a part of the gigabit network (Hakonen 2021).

4   LOCALIZATION

Simultaneous localization and mapping (SLAM) has been studied currently in simulated environment, paving the way for experimental software framework to be implemented within WP4 in T4.3 and tested on lab scale platforms within WP2 and WP6.

4.1   SLAM IMPLEMENTATION IN SIMULATED ENVIRONMENTS BY TALTECH

Environment
In the simulation, the whisker sensor array is modelled as a grid that is kept at the height of the whiskers. Like the screw driven robot platform, the grid can move holonomically. The environment the grid moves is set as an uneven terrain model, with different geometric shapes (cuboids, sphere, cylinder). Figure 41 shows the environment set-up with waypoints used to describe the movement in different scenarios.
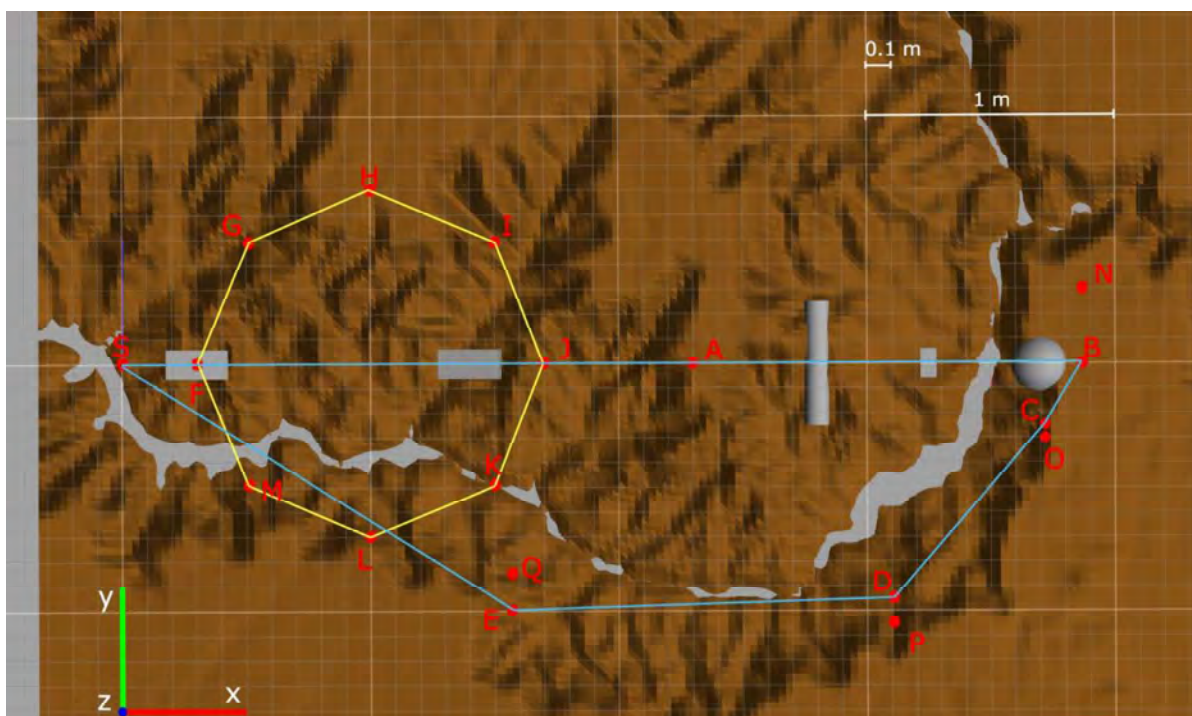

Figure 41 The uneven terrain with geometric shapes and waypoints on simulation map. The small and large loop denoted with yellow and teal lines respectively. Grid scale visible top right. Axes shown bottom left: red – x-axis, green – y-axis, blue – z-axis pointing upwards

During the movement, the simulated whisker sensor array publishes joint angles for each whisker sensor. The joint angles are transformed into inclination and azimuth angles, to match the data format of the physical sensor. A point cloud of contact points is generated assuming the whisker tip as a contact point with the environment from the published angles.

SLAM
The SLAM framework used in the simulated framework was modelled after those used for LIDAR (Laser Imaging Detection and Ranging) sensors; The whisker array resembles a LIDAR with a limited range and field of view. The algorithm used was based on the offline SLAM method using a 3-d LIDAR proposed in (Koide 2019). The method using whisker array can be used online due to the significantly smaller point cloud and small test environment.
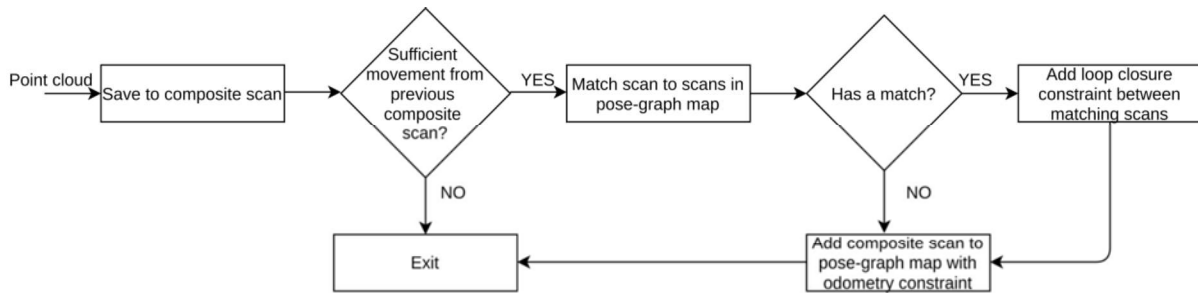
Figure 42 The flowchart of the modified SLAM algorithm used with whisker sensor grid.

The SLAM algorithm works by adding scans cumulatively to a point cloud until a criterion is reached, forming a key frame, which is added to the pose graph. Adding these scans to the composite scan is done based on odometry pose estimate. The criterion to add a composite scan to the map is fulfilled when, either the sensor position change in x or y dimension, or the heading angle change, crosses a threshold. This composite scan is matched with other composite scans in the map in the same manner as before. The flowchart showing the modified SLAM algorithm used with the whisker grid is given in Figure 42.

Results

The SLAM was evaluated for 5 different scenarios with varying complexity. The SLAM algorithm performed better than odometry in vehicle position estimation for all scenarios. This suggests improved localisation capabilities of the proposed model.
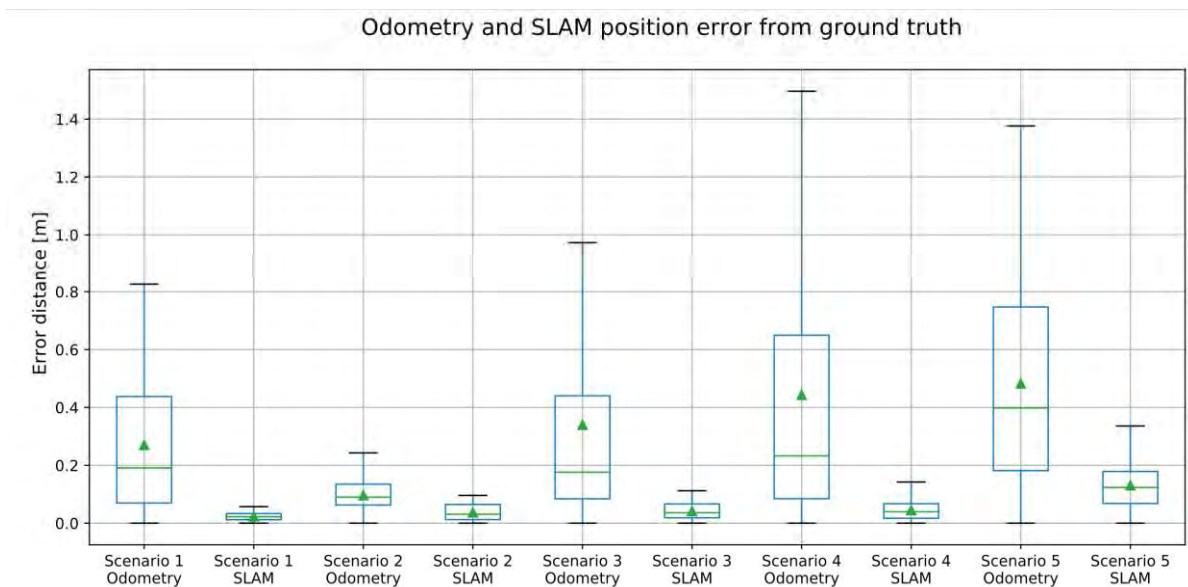

Figure 43 SLAM and odometry errors from ground truth during all 5 driving scenarios. The mean error is denoted with green triangle. Error distance calculated as Euclidean distance from x and y coordinates of robot.

In addition, the map representations produced by the algorithm were visually like the ground truth. The artificial objects (cuboids, cylinder, sphere) are visible for all scenarios. Furthermore, the uneven terrain features can also be seen on the resulting maps. Figure 43 shows the SLAM and odometry error in meters from the ground truth.

Next steps

The work on the SLAM algorithm will be continued. Next steps will be to test the SLAM algorithm using experimental data and integrating other sensor modalities to the SLAM framework.

5 PLANNED FUTURE EXPERIMENTS

The experimental work in the previous sections will be continued in various WPs. The list of different future experiments is summarized in the table below:

Table 3 List of future experiments with lab scale prototypes

Experiment	WP	Responsible partner	Partners involved	Time period	Connected WPs
Soil type detection through locomotion	WP 2	TalTech	TAU, RBINS	Aug-Oct 2021	WP4, WP6
Electrode array tests for mine mapping	WP6	RBINS	TalTech, TAU	Aug 2021- March 2022	WP2, WP4, WP7
Data gathering for offline SLAM testing	WP6	TalTech		Aug-Sept 2021	WP4, WP6
Whiskers based SLAM	WP6	TalTech	TAU, RBINS	March – April 2022	WP4, WP6
Testing final prototype screw module	WP3	TAU		Aug-Oct 2021	WP7,
Modularity tests for coping with failures					
Testing artificial hydraulic muscles	WP3	TAU		June-Dec 2021	WP7
Testing IMU and providing data of it	WP3	TAU		June-Aug 2021	WP7
Testing robustness of components under pressure	WP3	TAU		Aug 2021 –	WP7
Testing coupling unit, boom of the drilling unit	WP3	TAU	MUL	Sep 2021 -	
Modules locomotion	WP2	UPM		June 2021-end 2021	
Modules coupling mechanism	WP2	UPM		June 2021-end 2021	

The given list of experiments is not final and will be adjusted according to the findings of the experiments and the decisions made in various WPs.

6 CONCLUSION

The current report gave an overview of the work performed by M24 on lab scale prototypes for locomotion, sensing and localization. The presented results demonstrate the applicability of the technologies and lay groundwork for further investigations after the submission of this deliverable. More specifically, for the locomotion principal investigation, two indoor test tanks were assembled in Tampere and Tallinn, small scale prototype platforms along with test beds for configurability and components pressure tolerance test were assembled. For sensing investigation, a test platform was assembled for evaluating blind mapping using touch based sensors and additional IMU based odometry evaluation was performed. Additionally, mineral sensing testbeds for conductivity and LIBS spectrometry have been built. The localization within this work has been limited with simulated environments as the actual platforms for testing SLAM have become available just recently.

Although, this deliverable was postponed for 1 month, it should be taken into account, that more could have been achieved with the lab scale prototypes without the COVID-19 related restrictions to access into labs and for and visits among partners.

7   REFERENCES

Aaltonen, Jussi, Eetu Friman, Raphael Goossens, Kalle Hakonen, Kari Koskinen, Jouko Laitinen, Tuomas Salomaa, and Pirkka Ulmanen. 2020. "ROBOMINERS DELIVERABLE D3.2 ROBOT CONCEPTUAL DESIGN REPORT," 1–32.

Burlet, Christian, Giorgia Stasi, Michael Berner, Eva Hartai, Norbert Németh, Stephen Henley, Mike Mcloughlin, Tobias Pinkse, and Asko Ristolainen. 2020. "ROBOMINERS DELIVERABLE D6.1 MINER PERCEPTION REPORT," 1–44.

Hakonen, Kalle. 2021. "Testing Electronic Components and Systems under Hydrostatic Pressure," no. February. http://www.talkingelectronics.com/projects/Testing Electronic Components/TestingComponents.html#35.

Hartai, Éva, Norbert Németh, János Földessy, Steve Henley, Gorazd Žibret, and Krzysztof Galos. 2020. "ROBOMINERS DELIVERABLE 5.1."

Ristolainen, Asko, Maarja Kruusmaa, and Simon Godon. 2020. "ROBOMINERS DELIVERABLE D1.2 NEW NEW BIO-INSPIRED LOCOMOTION STRATEGIES CONCEPTS FOR."

Ristolainen, Asko, Laura Piho, and Maarja Kruusmaa. 2020. "ROBOMINERS DELIVERABLE D1.1 REPORT REPORT ON SENSOR PERFORMANCE AND NAVIGATION," 1–25.

Solomon, Joseph H., and Mitra J. Hartmann. 2006. "Robotic Whiskers Used to Sense Features." *Nature* 443 (7111): 525–525. https://doi.org/10.1038/443525a.

WP4. 2021. "ROBOMINERS Operational Scenarios."

8 APPENDICES

8.1 APPENDIX – 1 PRE-PROCESSED RESULTS FROM TALTECH TANK EXPERIMENTS

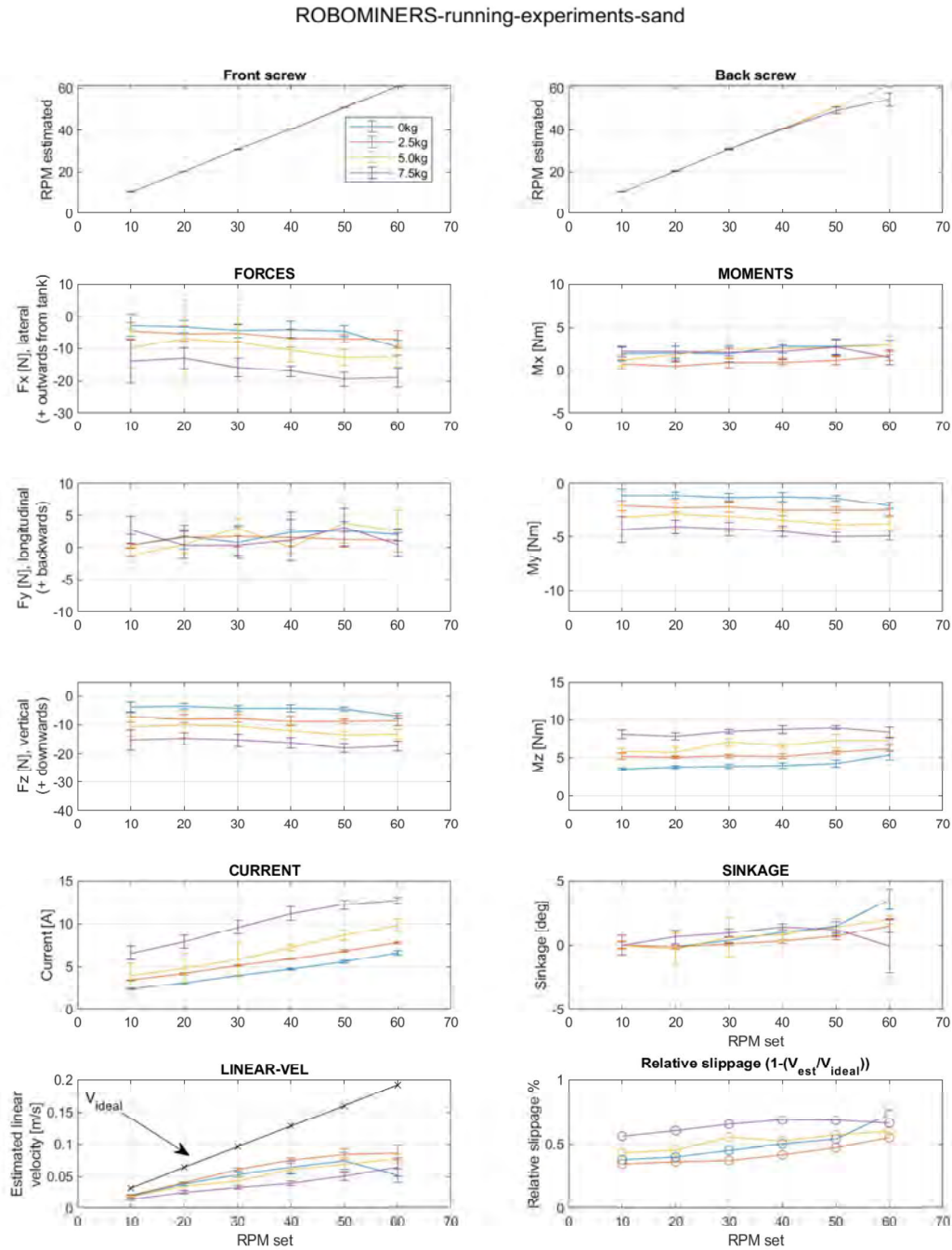**Free running experiments**

Figure 44 Early results from TalTech screw module tests: free running on sand
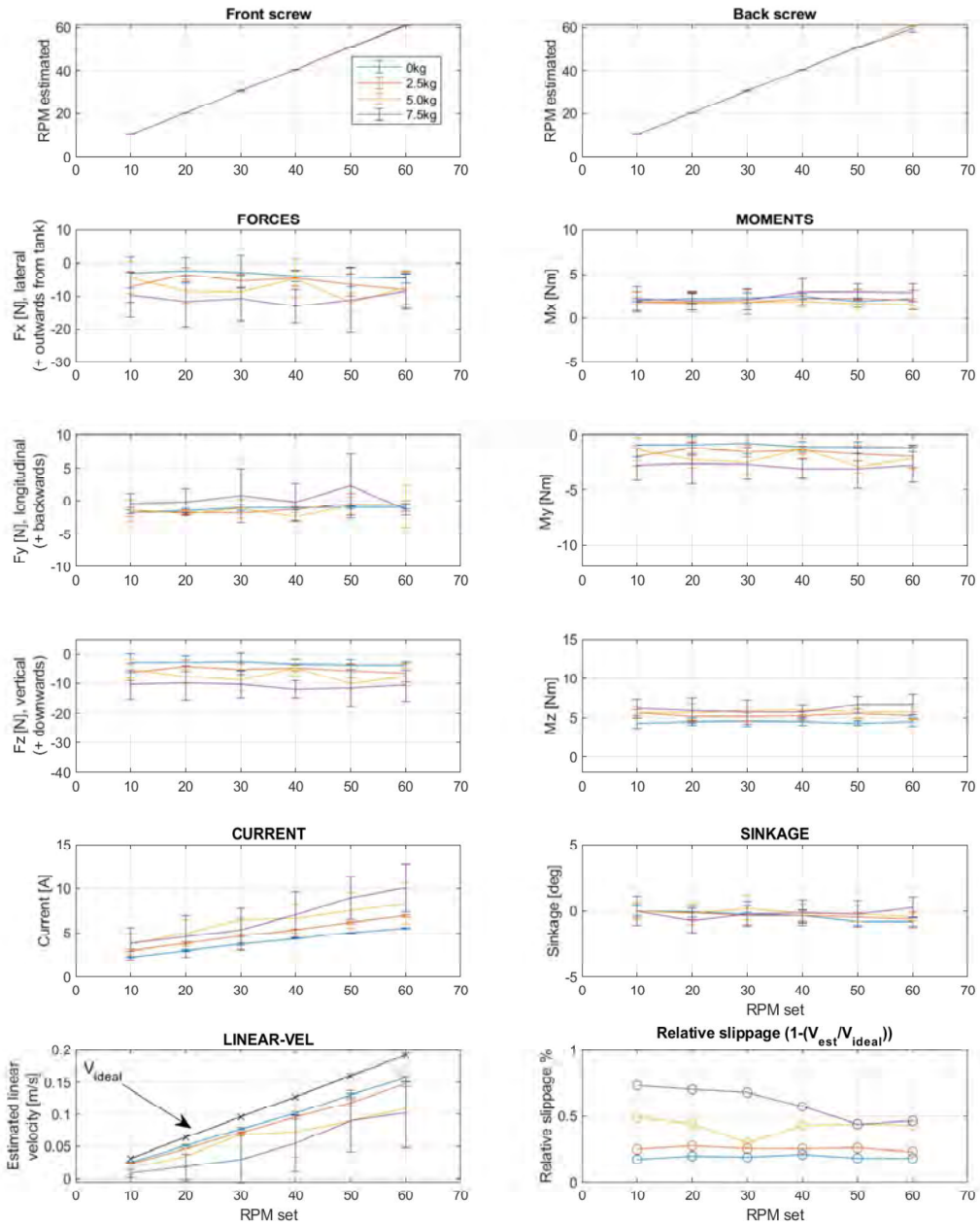
ROBOMINERS-running-experiments-wetsand

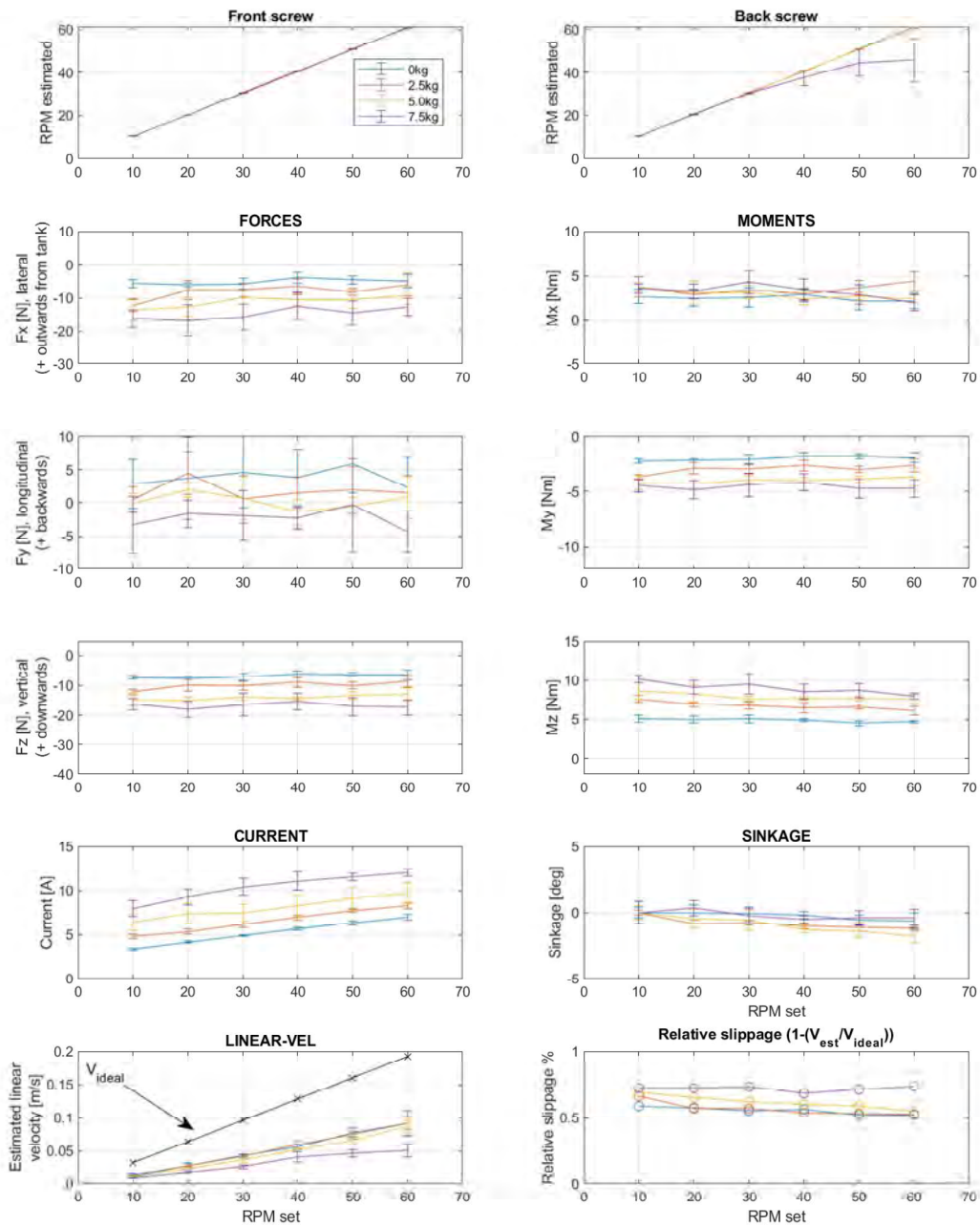Figure 45 Early results from TalTech screw module tests: free running on wet sand

Figure 46 Early results from TalTech screw module tests: free running on gravel

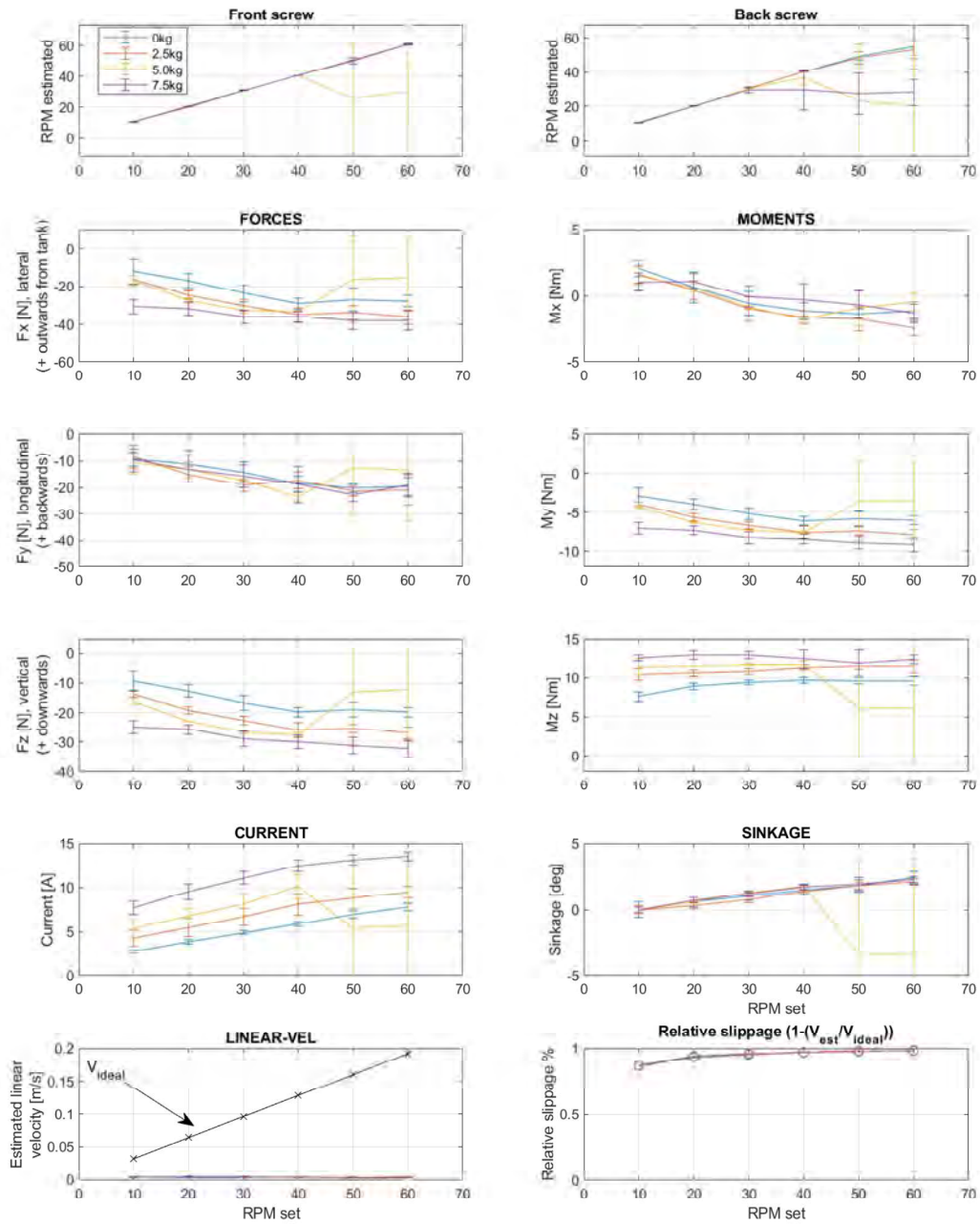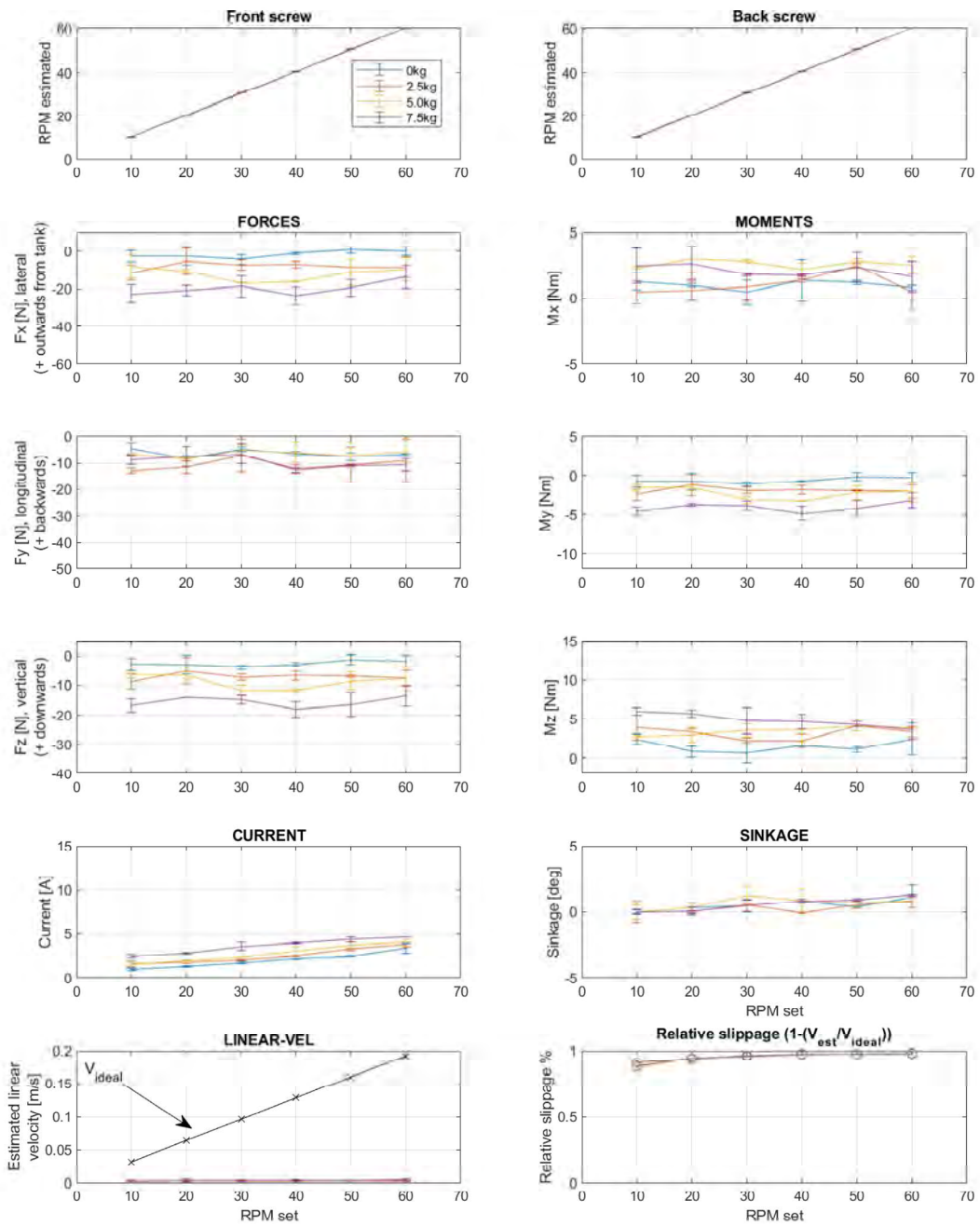Bungee pulling experiments

ROBOMINERS-bungee-experiments-sand

Figure 47 Early results from TalTech screw module tests: bungee on sand

Figure 48 Early results from TalTech screw module tests: bungee on wet sand
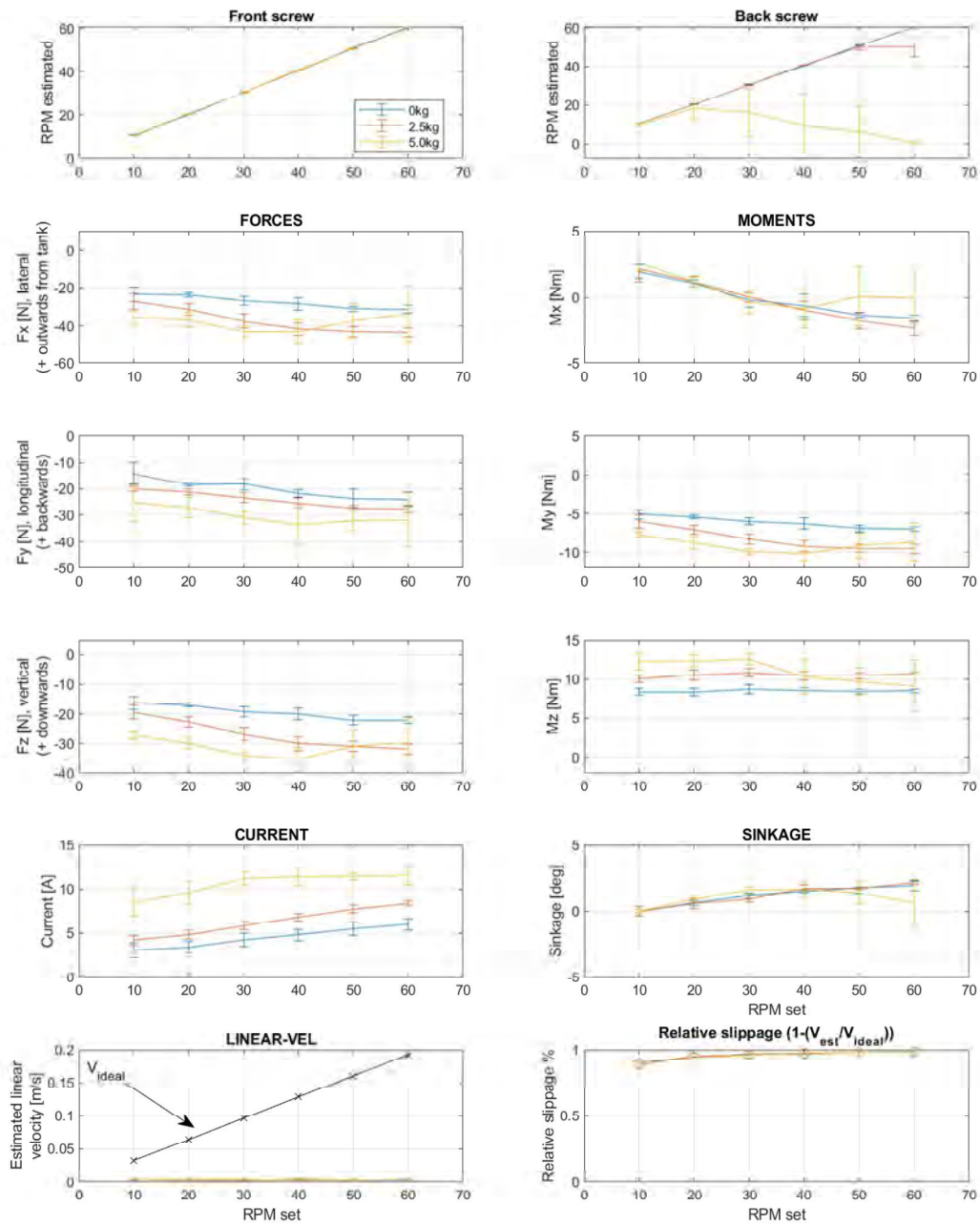
Figure 49 Early results from TalTech screw module tests: bungee on gravel

8.2   APPENDIX – 2 SLAM EXPERIMENTS
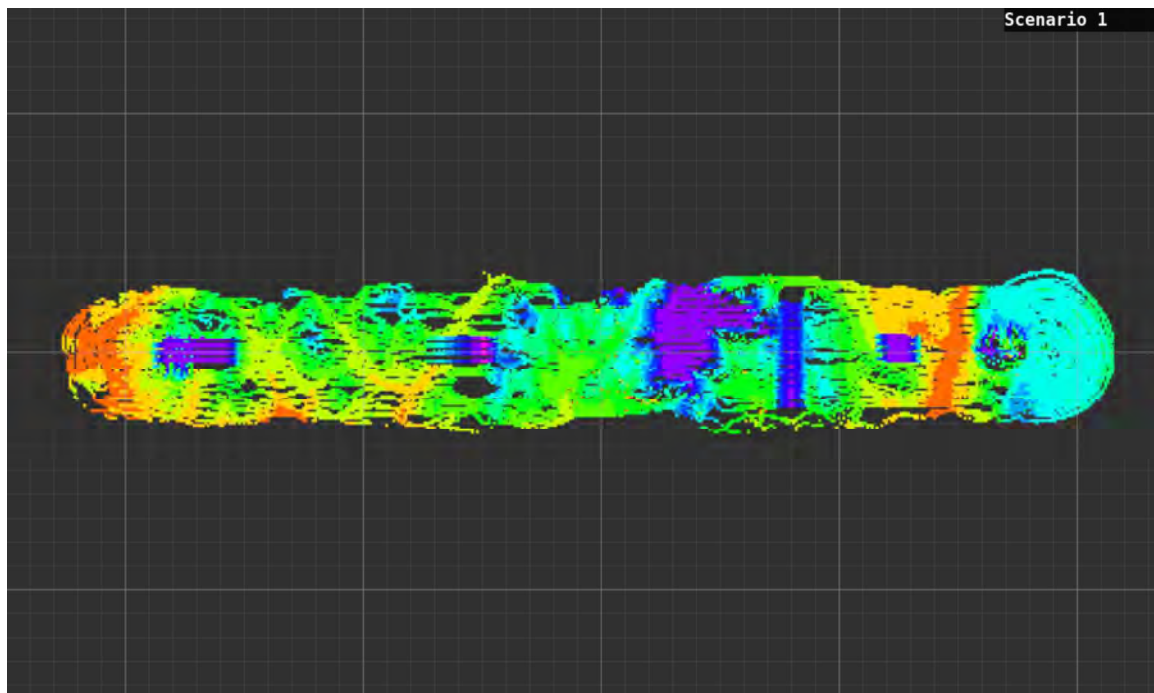
Figure 50 The results from scenario 1. Violet/blue - highest points, orange/red - lowest points. The objects are clearly visible on the height map, together with the uneven terrain features.
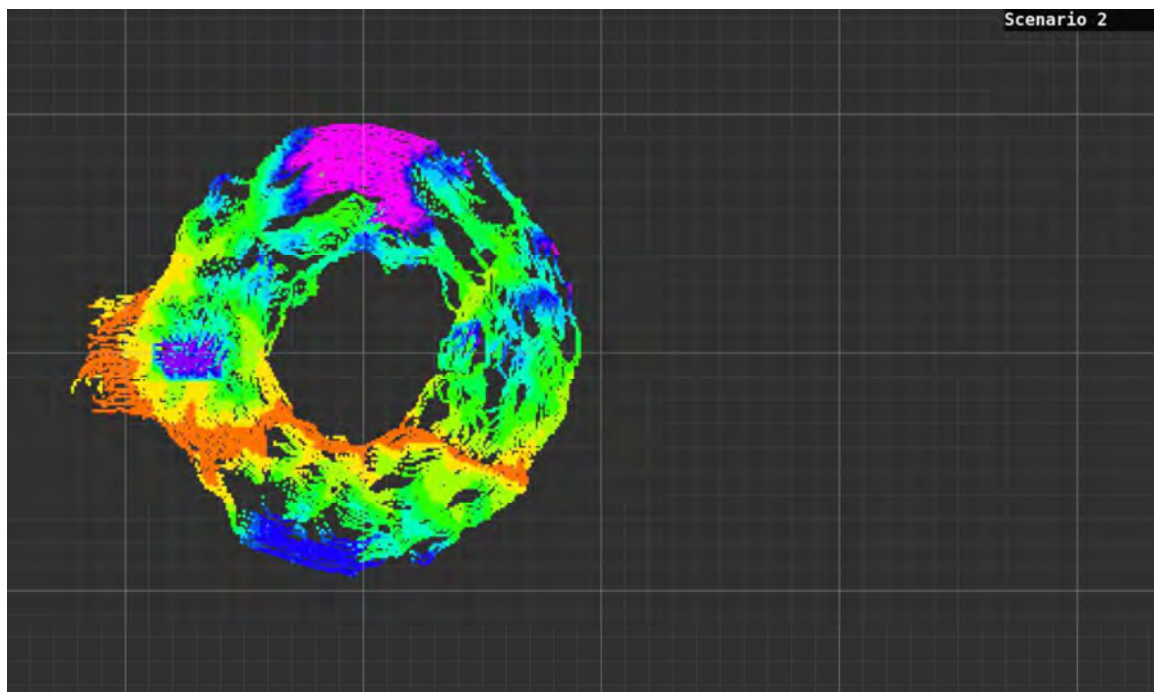

Figure 51 The results from scenario 2. Violet/blue - highest points, orange/red - lowest points. The first object (brick) is clearly visible on the height map. The second is object (slide) is barely visible, due to it being approached from the side, and the whiskers will slide off it, instead of crossing.
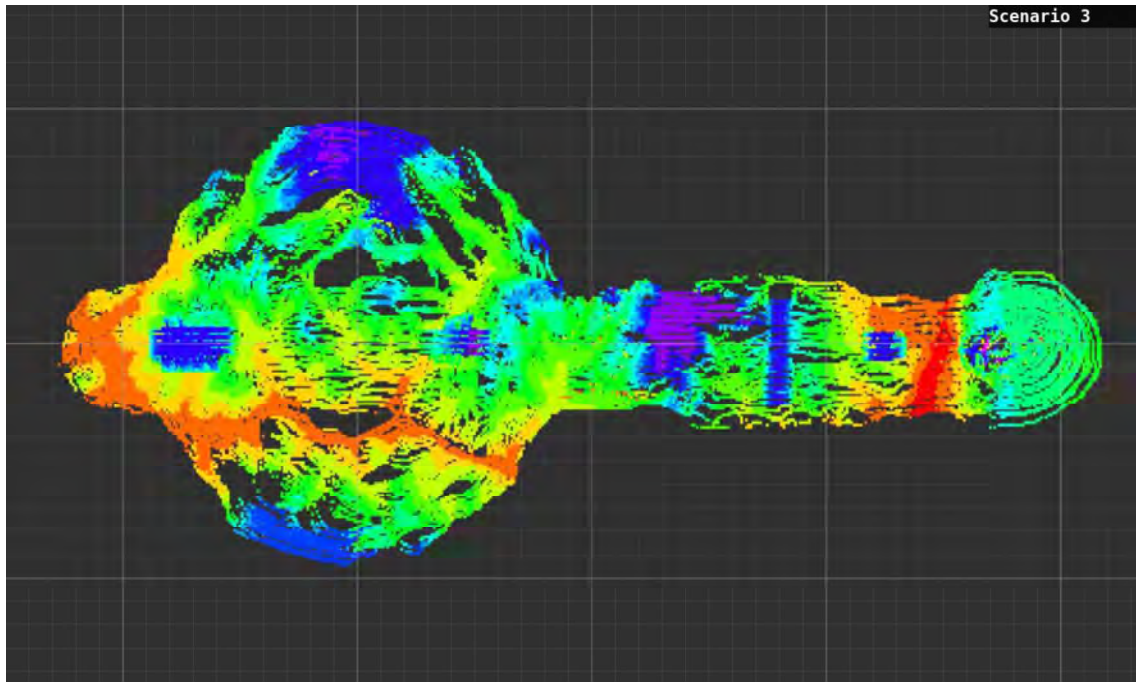
Figure 52 The results from scenario 3. Violet/blue - highest points, orange/red - lowest points. The objects and the terrain features are clearly visible on the height map. Even though the whiskers will slide off the sphere and the brick slide (when approached from the small circle), both objects are visible.
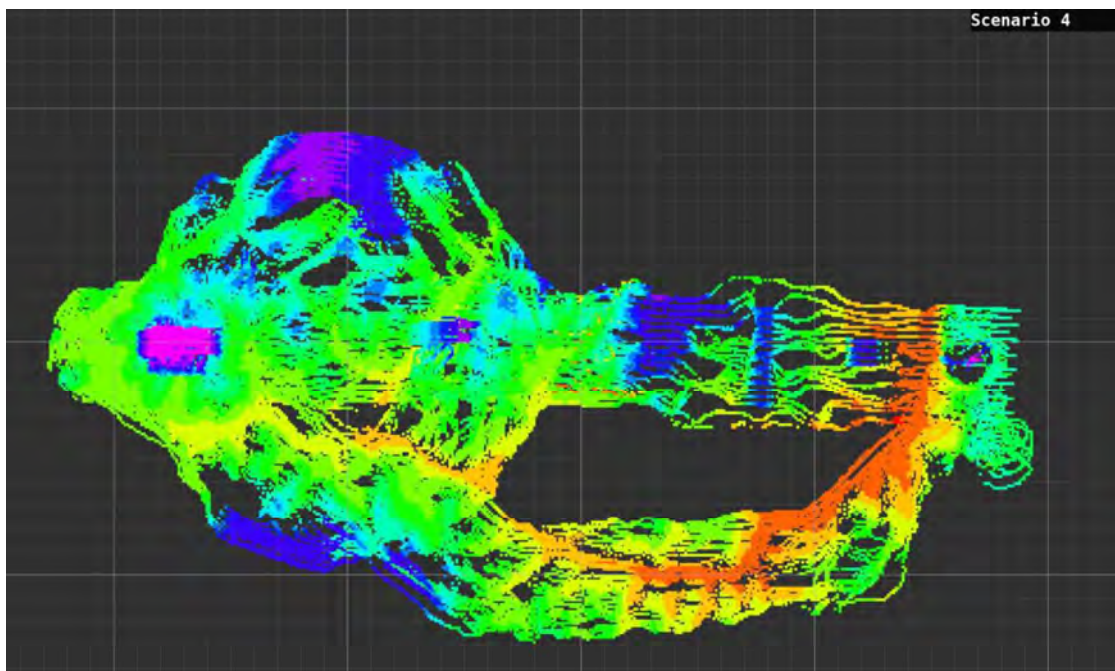

Figure 53 The results from scenario 4. Violet/blue - highest points, orange/red - lowest points. The objects and the terrain features are clearly visible on the height map. On the large loop, there are no objects, but the terrain features are visible.
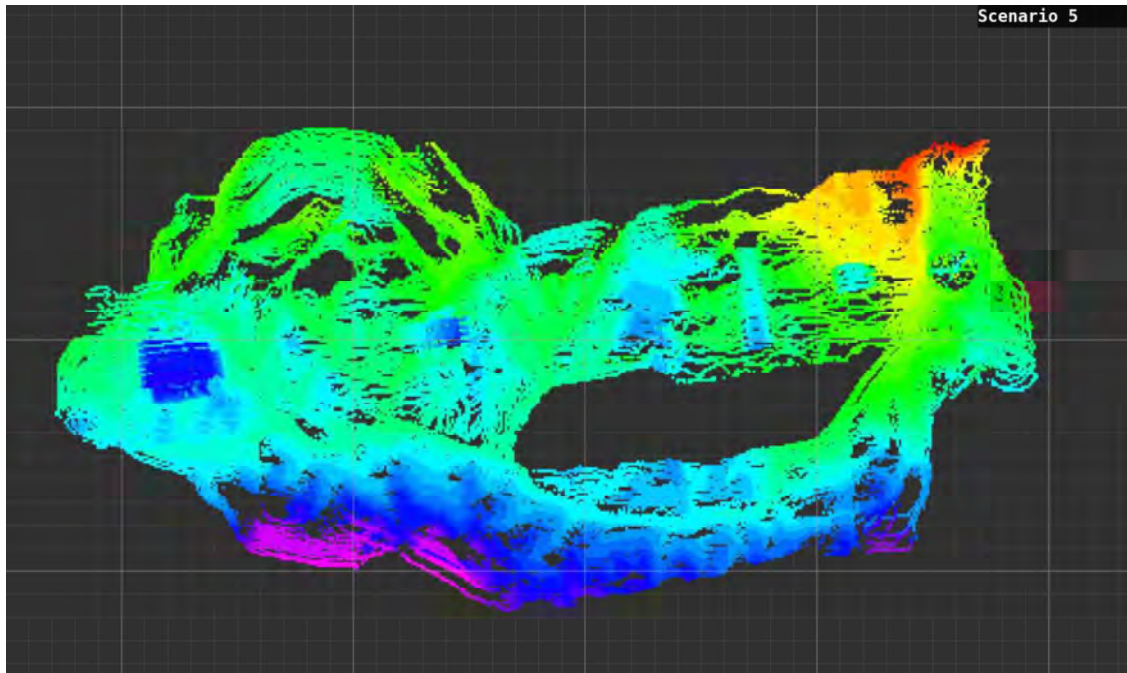
Figure 54 The results from scenario 5. Violet/blue - highest points, orange/red - lowest points. The objects and the terrain features are clearly visible on the height map. On the large loop, there are no objects, but the terrain features are visible. The whole map is slightly tilted.
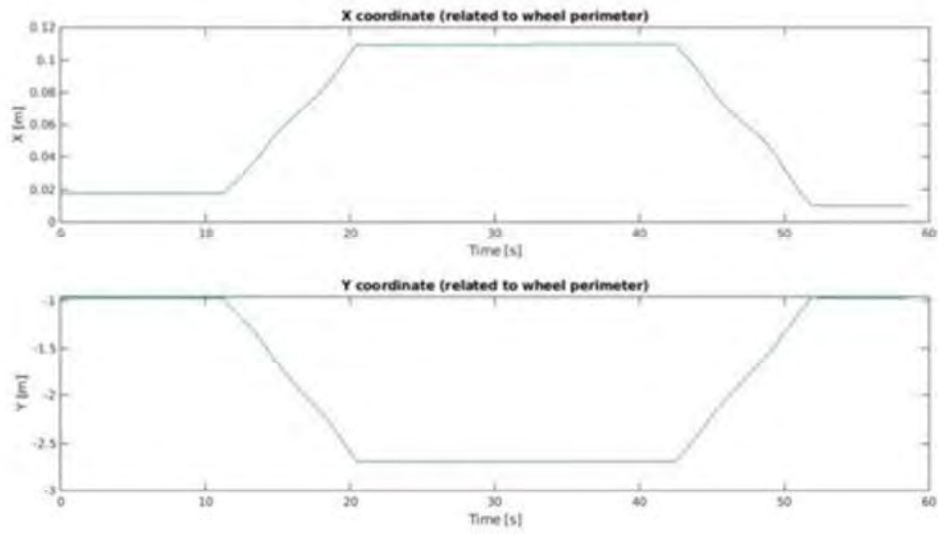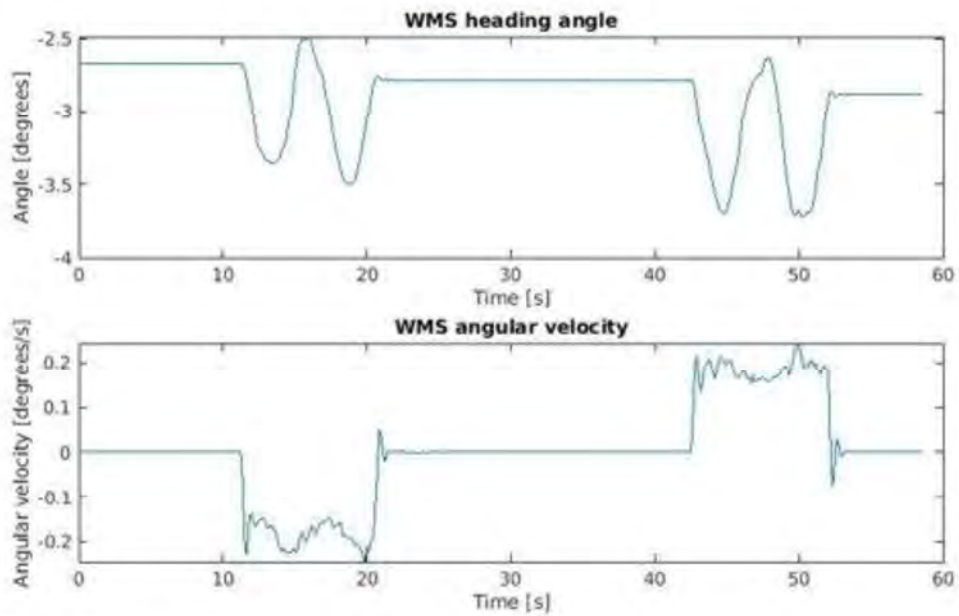
8.3 APPENDIX – 3 IMU TEST SAMPLES

Figure 55 WMS X and Y coordinates

Figure 56 WMS heading and velocity